

# **ILLINOIS TOLLWAY PROJECT**

**ILLINOIS TOLLWAY I-88 GROUND TIRE RUBBER TEST SECTIONS:**

**LABORATORY MIX DESIGNS & PERFORMANCE TESTING**

**BY**

**WILLIAM G. BUTTLAR**

Professor of Civil and Environmental Engineering

Glen Barton Chair in Flexible Pavements

University of Missouri-Columbia

**PUNYASLOK RATH**

Graduate Research Assistant

Department of Civil and Environmental Engineering

University of Illinois, Urbana-Champaign

September 22, 2017

# CONTENTS

EXECUTIVE SUMMARY .....	4
1. INTRODUCTION .....	5
2. PROJECT DESCRIPTION.....	5
3. EXPERIMENTAL PROCEDURE .....	6
3.1. Disk-Shaped Compact Tension Test (DC(T)).....	7
3.2. Hamburg Wheel Tracking Test.....	9
3.3. Performance-Space Diagram .....	10
3.4. Illi-TC Modeling.....	11
4. RESULTS AND DISCUSSIONS.....	11
4.1. Disk-Shaped Compact Tension Test.....	11
4.2. Hamburg Test Results.....	17
4.3. Performance-Space Diagram .....	18
4.4. Illi-TC Results.....	19
4.5. Acoustic Emission Test Results.....	20
5. CONCLUDING REMARKS.....	21
6. REFERENCES .....	22
Appendix A: DC(T) Creep Compliance .....	24
Appendix B: Acoustic Emission Testing .....	35
Appendix C: Post-Cracking Correction Factor.....	39
Appendix D: Remaining Sample Inventory.....	43
Appendix E: Mix Designs.....	44

## LIST OF TABLES

Table 1. Summary of GTR Technologies and Asphalt Binder Types .....	6
Table 2. Location of GTR Test Sections on Reagan Memorial Tollway (I-88) .....	6
Table 3. Summary of DC(T) Fracture Energy Results .....	12
Table 4 . Critical Events count from Illi-TC runs for plant-compacted gyratory samples.....	20
Table 5. Critical Events count from Illi-TC runs for field cores.....	20
Table 6. m-value for plant-compacted gyratory samples.....	27
Table 7. Damage percentages of plant-compacted gyratory mixes .....	29
Table 8. Creep load levels for different field cores.....	30
Table 9. m-value for field cores .....	32
Table 10. Damage percentages of field cores .....	34
Table 11. Acoustic Emission Testing - Embrittlement Temperatures for mixes .....	38

## LIST OF FIGURES

Figure 1. Loading Fixture for Disk-Shaped Compact Tension Test.....	7
Figure 2. Typical load-CMOD curve from DC(T) testing of asphalt mixtures .....	8
Figure 3. DC(T) specimen dimensions (ASTM D7313-13) .....	8
Figure 4. Fabricated DC(T) specimen from the plant-compacted gyratory sample.....	9
Figure 5. Hamburg Wheel Tracking Device: a) During test b) After test.....	10
Figure 6. Performance-Space Diagram .....	10
Figure 7. Illi-TC data input .....	11
Figure 8. Fracture energies for plant-produced gyratory samples .....	13
Figure 9. Fracture energies for field cores .....	14
Figure 10. Effect of additives on fracture energy for particular binders.....	15
Figure 11. Comparison of fracture energies for field cores and plant-compacted gyratory samples for -12°C.....	16
Figure 12. Comparison of fracture energies for field cores and plant-compacted gyratory samples for -18°C.....	17
Figure 13. Hamburg Wheel Tracking Test .....	18
Figure 14. Performance-Space Diagram.....	19
Figure 15. 2-D elastic model to simulate DC(T) Creep.....	25
Figure 16. Master curve for GTR mixes (gyratory samples).....	26
Figure 17. Master curve for Elastiko (ECR) mixes (gyratory samples).....	26
Figure 18. Master curve for Evoflex (RMA) mixes (gyratory samples).....	27
Figure 19. a) DC(T) fracture energy values after creep testing b) DC(T) fracture energy test results without any creep compliance testing (Test temperature = -12°C).....	28
Figure 20. Creep compliance master curve for GTR field cores .....	31
Figure 21. Creep compliance master curve for Elastiko (ECR) field cores.....	31
Figure 22. Creep compliance master curve for Evoflex (RMA) field cores .....	32
Figure 23. a) DC(T) fracture energy values after creep testing for field cores b) DC(T) fracture energy test results for field cores without any creep compliance testing .....	33
Figure 24. Working concept of Acoustic Emission Method[18] .....	35

Figure 25. Typical AE plot [18].....	36
Figure 26. Embrittlement temperatures of field cores from AE testing.....	37
Figure 27. Embrittlement temperatures of gyratory samples from AE testing .....	37
Figure 28. DC(T) specimens, a) standard specimen with notch length = b, b) non-standard specimen with notch length = b1 .....	39
Figure 29. Typical Load-CMOD curve showing crack propagation stages.....	40
Figure 30. General correction factor function.....	41
Figure 31. Load-CMOD plot with and without correction factor .....	42

## EXECUTIVE SUMMARY

The usage of Ground Tire Rubber (GTR) in asphalt mixtures is advantageous for the state of Illinois, as it imparts performance benefits such as better cracking and rutting resistance, along with environmental benefits. Extensive research has been performed on GTR-modified asphalt in recent years, resulting in advancements in previous GTR technologies. This project investigates two relatively new GTR technologies- Elastiko 100 Engineered Crumb Rubber (ECR), and Evoflex Rubber Modified Asphalt (RMA), along with a terminal-blend GTR product from Seneca Petroleum that has been used on the Tollway for nearly a decade. The ECR technology is an engineered crumb rubber that can be added to the hot mix asphalt plant through the RAP collar, which can be considered as a new, fine-grind dry-process GTR approach. The ECR product is engineered to readily release from transport vehicles, and imparts workability into the modified mixture. Evoflex RMA comes in pellet form, and is engineered with GTR, SBS and other additives to enhance workability. The terminally-blended GTR product has led to good-performing field sections on the Tollway, with >330,000 mix tons placed with this product over the past decade in the Chicagoland area. An experimental matrix considering various levels of asphalt binder replacement resulting from the use of reclaimed asphalt pavement (RAP) and recycled asphalt shingles (RAS) and two different base binders was established, with a total of 9 mixtures investigated.

Phase-I of the project consisted of testing to determine the low-temperature cracking characteristics of the mixes, which were designed by S.T.A.T.E. Testing, LLC. Plant-compacted gyratory samples and field cores were sampled and tested to measure their fracture energy using the Disk-Shaped Compact Tension (DC(T)) test at two temperatures (-12°C and -18°C). The lowest fracture energy value measured among the nine mixtures at the standard test temperature of -12°C was 688 J/m<sup>2</sup>, which demonstrates the high degree of thermal cracking resistance that can be expected with all three technologies. Hamburg Wheel Tracking test results were obtained from S.T.A.T.E. Testing LLC., and DC(T)-Hamburg plots were used as a graphical tool for mix evaluation based on low-temperature cracking and rutting potential. The plots revealed that all the mixes would perform well in the field. In addition, the alignment of the data on a relatively straight line demonstrates the advantage of pairing the Hamburg with the DC(T) as bookend performance tests; namely, that mix designers can use this relationship to expedite mix design testing. Further, Acoustic Emission testing (Appendix B) was also conducted with all the mixes to determine the embrittlement temperature. The results show that Elastiko and Evoflex have a similar effect on the embrittlement temperatures while the Seneca GTR mixes showed the coolest embrittlement temperatures. AE testing on gyratory samples reveal that the use of a softer binder decreases the embrittlement temperature, and the addition of recycled material increases it, as expected.

Phase-II of the project consisted of creep compliance testing using the DC(T) set-up, after conducting research to develop this new technique. Creep compliance curves were obtained at 0°C, -12°C, and -24°C for each mixture type. A Generalized Voigt-Kelvin Model was regressed onto the resulting master curves, with -24°C selected as the reference temperature. The obtained master curves were smooth with very reasonable shift factors, and ranking of master curves with variation in mixture properties were as expected. Immediately after the final creep compliance test was completed, the specimens were fractured at the same temperature. The creep compliance test is generally assumed to be non-damage inducing. However, the obtained fracture energy values of the samples subjected to creep compliance testing were lower than those that were only subjected to fracture testing. This research has led to improvement and finalization of the new creep testing protocol for the DC(T). Further research will be conducted to develop a standard specification that helps ensure that no significant damage occurs during creep tests in the event that specimens are to be tested in both creep and fracture.

Finally, a thermal cracking model – Illi-TC, developed by Dr. Eshan Dave under the guidance of Dr. W.G. Buttlar at the University of Illinois at Urbana-Champaign, was utilized to predict the thermal cracking potential of the 9 study mixtures. The mixtures were to be free of thermal cracking throughout their service life, as zero thermal cracking potential was predicted for all 9 mixes using the simulation software.

## 1. INTRODUCTION

The United States has a long history of using Ground Tire Rubber (GTR) in the construction of asphalt pavements. The Federal Highway Administration (FHWA) has been involved in ‘rubber technology’ since the 1970’s, and throughout the 1980’s it reported on a number of asphalt-rubber paving technologies. For instance, the FHWA released a report in 1992 detailing the design and construction of asphalt paving materials with Crumb Rubber Modifier (CRM)<sup>1</sup>. The report describes benefits of CRM modifiers, such as increased thermal and reflective cracking resistance, increased rutting resistance, improved overall durability, and increased asphalt-aggregate adhesion [1]. There were reports of a mixed performance by the rubber-modified pavements by various DOTs in the 1980s-1990s, but since then the GTR technology has undergone transformations and tens of millions of tons have been placed with success across the US on interstate highways and other important paving projects [2]. The initial failures could be attributed to the faulty specifications, material selection, and quality control in the field. In some cases, rubber particles segregated/settled in the binder during storage leading to the formation of lumps in the binder. This would often lead to premature cracking in early rubber-modified pavements. Early GTR-modified mixtures also posed a challenge to contractors owing to their inexperience in handling materials with decreased workability [3]. As paving agencies gained more experience in handling GTR-modified materials, better specifications were put in place and subsequently, the performance of GTR-modified pavements improved.

GTR-modified asphalt binder has been extensively studied and researched. A study conducted by Richard et al. [4] examined the effect of particle size, surface area, and grinding method of the GTR on the asphalt binder. Their study also examined the performance of a polymer-modified asphalt rubber mix. Xu et al. conducted a rheological investigation on the effects of additives like PPA, EVA, elastomers, and plastomers in GTR-modified asphalt [5]. Vahidi et al. studied the effect of GTR and treated GTR on high-RAP mixes. The study included results from a host of mix and binder tests, such as Hamburg, multiple stress creep and recovery, mix stiffness ( $E^*$ ), Texas overlay test, etc. GTR-modification has been used with different binder systems as well as with other additives [6]. Williams et al. looked into a rubber-modified bio-asphalt [7]. Akisetty et al. examined the high-temperature properties of GTR-modified binders with two WMA additives [8], while Chui et al. conducted a performance evaluation of asphalt rubber SMA [9].

The current study compares two GTR technologies being considered by the Illinois Tollway, namely, Elastiko 100 Engineered Crumb Rubber (ECR) and Evoflex Rubber Modified Asphalt (RMA), alongside the more commonly used terminal-blend GTR process.

## 2. PROJECT DESCRIPTION

The Illinois Tollway constructed test sections for three Ground Tire Rubber<sup>1</sup> (GTR) asphalt modifier technologies on the Reagan Memorial Tollway (I-88) in April 2016. Apart from estimating the performance characteristics of the new GTR technologies, the study also examined the effect of softer virgin binder and an increased amount of reclaimed asphalt on mix performance properties. Accordingly, the GTR technologies were incorporated into SMA mixes with 33% asphalt binder replacement (ABR) using a ‘standard’ base or virgin binder (PG 58-28) and a softer base binder (PG 46-34). A third design was also used, where the softer base binder was combined with an increased asphalt binder replacement (ABR) percentage (PG 46-34 with 47% ABR), obtained by increasing the content of recycled asphalt shingles (RAS). The mixture matrix is shown in Table 1.

---

<sup>1</sup>The FHWA uses the terminology CRM instead of GTR

Table 1. Summary of GTR Technologies and Asphalt Binder Types

<b>SMA Mixture Matrix for I-88</b>				
<b>All mixtures use the same base design aggregates</b>				
<b>Product</b>	<b>Binder</b>	<b>Base Binder</b>	<b>Softer Binder</b>	<b>Softer Binder &amp; Increased ABR</b>
<b>Seneca GTR</b>		PG 58-28 + 12% GTR	PG 46-34 + 12% GTR	PG 46-34 + 12% GTR & increase ABR
<b>Elastiko ECR</b>		PG 58-28 + 10% ECR	PG 46-34 + 10% ECR	PG 46-34 + 10% ECR & increase ABR
<b>Evoflex RMA</b>		PG 58-28 + 10% RMA	PG 46-34 + 10% RMA	PG 46-34 + 10% RMA & increase ABR
<b>ABR (%)</b>		33.9	33.9	46.8 (47.0 for Evoflex RMA mixture)
<b>Virgin Binder (%)</b>		4.03	4.03	3.21 (3.18 for Evoflex RMA mixture)
<b>Recycled Binder (%)</b>		2.07	2.07	2.82
<b>RAP in mixture blend (%)</b>		12.1	12.1	16.2
<b>RAS in mixture blend (%)</b>		5.0	5.0	7.0

In total, 12 field cores of 150 mm diameter were taken from each of the test sections for the nine mixes for evaluation by the research team. The core locations are shown in Table 2. Additionally, gyratory-compacted specimens, a minimum of 12 for each mix, were compacted by State Testing, LLC using as-produced mix sampled at the Curran Contracting Company asphalt plant in DeKalb, IL. Furthermore, loose mix, binders, and aggregates were sampled. The complete inventory list of remaining samples is shown in Appendix D.

Table 2. Location of GTR Test Sections on Reagan Memorial Tollway (I-88)

Rubber Modifier	Modifier Mile Post Limits			Individual Test Section Mile Post Delineations		
	Lane	Mile Post Start	Mile Post End	PG 58-28 Base Asphalt Liquid	PG 46-34 Base Asphalt Liquid	PG 46-34 Base Asphalt Liquid & High ABR
Evoflex RMA	EB Outside shoulder	65.2	66.0	65.2-65.5	65.5-65.8	65.8-66.0
Elastiko 100	EB Inside Lane (Lane 1)	60.1	61.3	60.1-60.5	60.5-60.9	60.9-61.3
Seneca GTR	EB Inside Lane (Lane 1)	64.4	66.2*	64.4-64.7	65.5-65.9	65.9-66.2

\* No GTR asphalt placed between Mile Posts 64.7 and 65.5

### 3. EXPERIMENTAL PROCEDURE

In Phase-I of the project, the low-temperature cracking performance was assessed through conducting the Disk-Shaped Compact Tension Test (DC(T)). The DC(T) test was performed on both field cores as well as the plant-compacted gyratory specimens. The specimens were tested at two different temperatures, the standard test temperature in the DC(T) for Illinois of -12°C and at -18°C, which is technically the correct test temperature for the northern Illinois climate following the LTPPBind software program for 98% reliability.

Phase-II of the project consisted of creep compliance testing using DC(T) machine and modeling the collected data in Illi-TC, the thermal cracking simulation tool developed at the University of Illinois. Creep compliance tests were performed only on plant-compacted asphalt mixture gyratory samples at 0°C, -12°C, and -24°C. All of the results for the DC(T) creep compliance testing are included in Appendix A.

### 3.1. Disk-Shaped Compact Tension Test (DC(T))

The DC(T) test was developed to characterize the fracture behavior of asphalt concrete materials at low temperatures. The testing temperature is 10°C warmer than the PG low temperature grade of the mixture, per ASTM D7313-13 [10]. Thermal cracking in asphalt pavements can be considered as occurring in pure tensile opening or fracture Mode I, as the cracks propagate perpendicular to the direction of the thermal-induced stresses in the pavement, i.e., transverse to the direction of traffic. For Mode I cracking, Wagoner et al. (2005) determined a geometry for the asphalt concrete (AC) specimen using ASTM E399 as a starting point, and the results obtained with this specimen geometry were very repeatable. Shortly thereafter, the DC(T) test for asphalt concrete was formalized into ASTM D7313-06, and has been updated several times since, including an Illinois-modified DC(T) procedure.

The DC(T) test procedure includes conditioning of the fabricated specimen at the selected test temperature in a temperature-controlled chamber for a minimum of two hours. After the conditioning, the specimens are suspended on loading pins in DC(T) machine, shown in Fig. 1. The test is performed at a constant Crack Mouth Opening Displacement (CMOD) rate, which is controlled by a CMOD clip-on gage mounted at the crack mouth. The CMOD rate specified in ASTM D7313-13 is 0.017 mm/s (1 mm/min). At the test temperature, a seating load no greater than 0.2 kN (typically about 0.1 kN) is applied before starting the test. The test is completed when the post-peak load level has reduced to 0.1 kN. The fracture energy can be obtained by measuring the area under the load-CMOD curve and dividing it by the fractured area (ligament length times thickness). A typical load-CMOD curve is shown in Fig. 2.

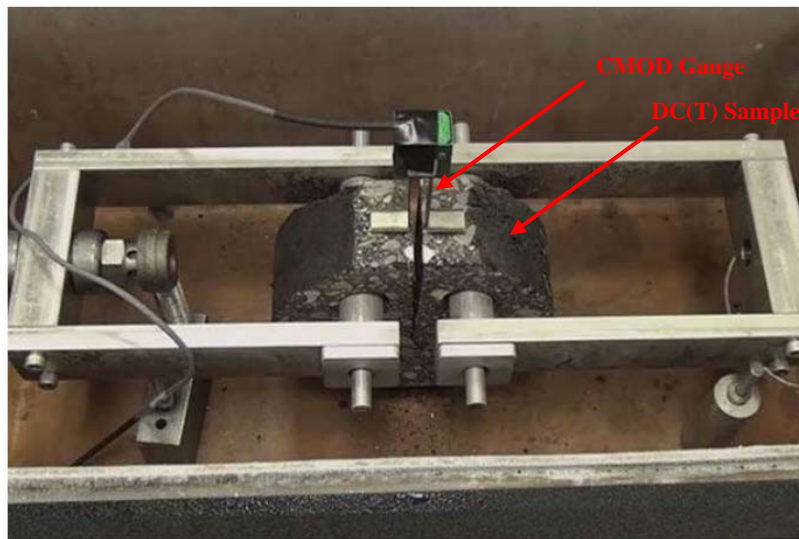


Figure 1. Loading Fixture for Disk-Shaped Compact Tension Test



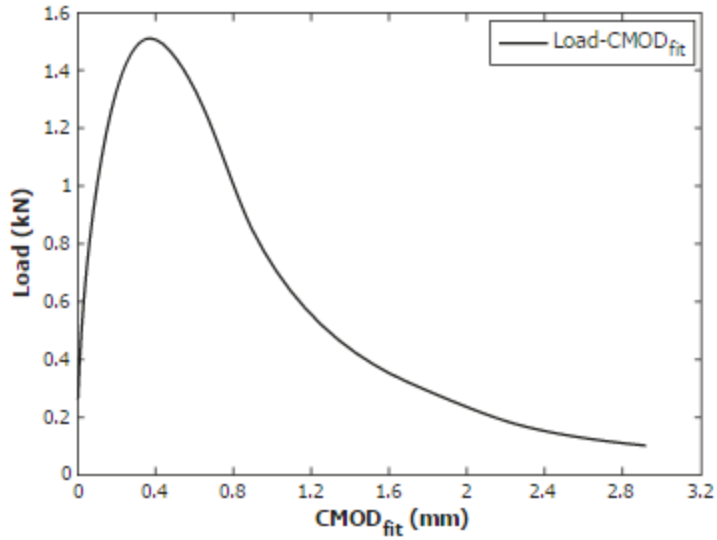


Figure 2. Typical load-CMOD curve from DC(T) testing of asphalt mixtures

It is important to mention that a correction factor was used in the calculation of the DC(T) fracture energy for some specimens to compensate for the deviation from the dimension specification of ASTM D7313-13. Fig. 3 shows the dimension of the DC(T) specimen according to ASTM D7313 and Fig. 4 shows a plant-produced specimen fabricated at UIUC. The fabrication error was caused by a temporary calibration error in a newly installed chop saw at the UIUC laboratory, which affected one set of the specimens tested and required a small correction factor to be applied.

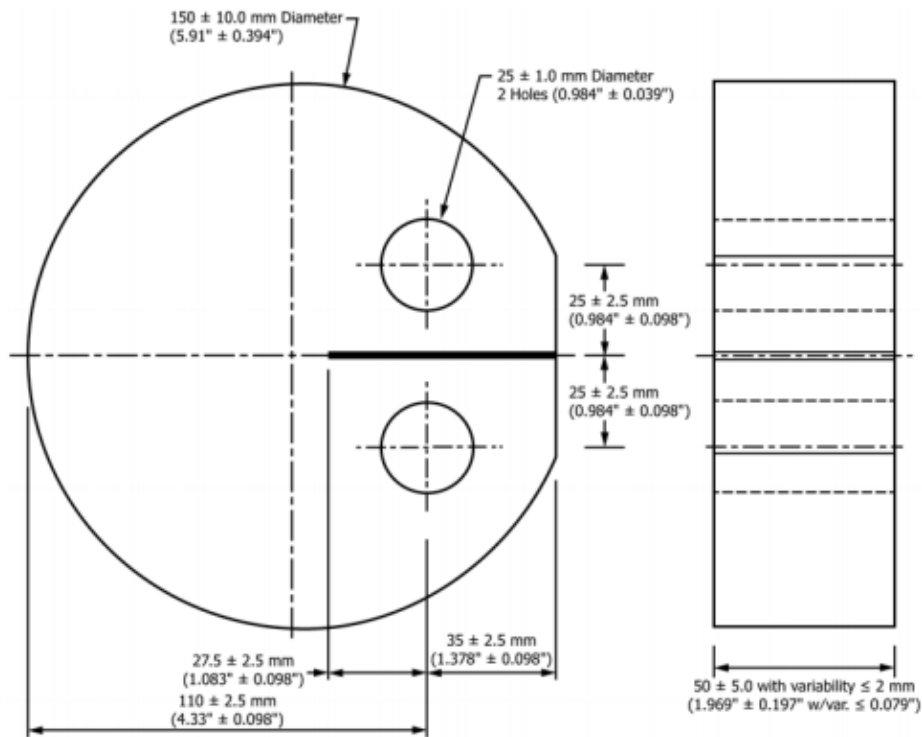


Figure 3. DC(T) specimen dimensions (ASTM D7313-13)



Figure 4. Fabricated DC(T) specimen from the plant-compact gyratory sample

A correction factor was calculated based on the fact that the CMOD rate is constant in the DC(T) test. A smaller notch would essentially prompt the loading assembly to ramp up the load to maintain the CMOD opening rate. However, after a certain point post-peak, the correction factor should trend to unity (1.0). The mathematics related to the correction factor is fairly simple and is shown in Appendix C. Under normal circumstances, specimens can be fabricated within the tolerances of ASTM D7313 and a correction factor is not needed.

The research team at UIUC conducted DC(T) tests on plant-compact gyratory samples as well as field cores from the nine different mixes. The DC(T) test temperature generally used in Illinois is  $-12^{\circ}\text{C}$  because PG64-22 is a commonly used binder grade in Illinois and the ASTM specifications state that DC(T) testing should be done  $10^{\circ}\text{C}$  warmer than the low temperature PG binder grade of the mix. As mentioned earlier, the UIUC team conducted the test at both  $-12^{\circ}\text{C}$  and  $-18^{\circ}\text{C}$  for research purposes. A minimum fracture energy threshold of  $690 \text{ J/m}^2$  was used as a criteria for the SMA mixes (high traffic volume road), in accordance to the recommendations of Marasteanu et al. (2007) in the National Pooled Study on Low Temperature Cracking, Phase-II.

### 3.2. Hamburg Wheel Tracking Test

The Hamburg Wheel Tracking Device, originally developed in Hamburg, Germany in the mid-1970, has been extensively used in North America as a mixture evaluation tool. The Hamburg Wheel Tracking test indicates both the rutting susceptibility and moisture sensitivity of the mix. It does so by tracking a loaded steel wheel repeatedly across submerged asphalt mixture specimens. Hamburg testing is conducted in a  $50^{\circ}\text{C}$  water-bath, as specified by AASHTO T-324. A loaded steel wheel, weighing approximately 71.7 kg, tracks over the samples in the heated water bath (Fig. 5). The deformation of the specimen is measured as a function of the number of passes. The test is stopped at 20,000 passes or once the rut depth reaches 20 mm. Tollway specifications require a rut depth of less than 6.0mm at 20,000 passes for SMA mixes. This test was completed by S.T.A.T.E Testing, LLC, and the results are reported herein.



Figure 5. Hamburg Wheel Tracking Device: a) During test b) After test

### 3.3. Performance-Space Diagram

Buttlar et al. (2016) used the DC(T) and Hamburg results to develop a graphical tool that gives a holistic idea of the overall performance of the mix [11]. Hamburg results are plotted on a reverse Y-axis arithmetic scale, while the DC(T) results are plotted on a standard arithmetic X-axis. The plot can be divided into four major parts- an upper-left section where the mix displays good rutting resistance but poor fracture energy, a lower-left section where the mix exhibits failure in both rutting and fracture, a lower-right section where the mix has suitable fracture energy but poor rutting resistance, and an upper-right section where the mix possesses good rutting and cracking resistance (Fig. 6). An ideal mix would lie in the upper-right corner of the performance-space diagram, which is especially critical for SMA mixtures. Although Tollway SMA's are required to have lower Hamburg rut depths, the standard Hamburg-DC(T) plot was used, which displays a line at the 12.5 mm rutting level.

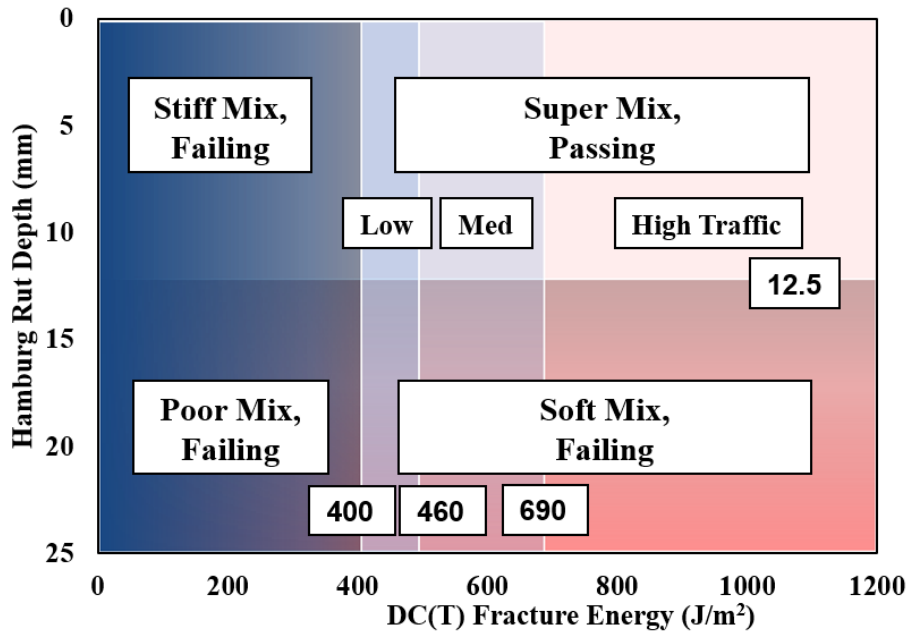


Figure 6. Performance-Space Diagram

### 3.4. Illi-TC Modeling

Illi-TC is a thermal cracking simulation tool developed by Dr. Eshan Dave, as part of Dr. Buttlar’s research group. The tool implements a viscoelastic finite element model with a 2D, cohesive zone fracture modeling approach. The model takes into account various parameters indicating the strength, relaxation, climatic, and mixture properties. The present version of Illi-TC has built-in sets of temperature profiles from different locations. The user inputs the thickness of the asphalt layer, its fracture energy, and the IDT tensile strength. Optionally, the tensile strength can also be computed from DC(T) peak load information. Further, the user is prompted to input either both - Void in Mineral Aggregate (VMA) and aggregate CTEC (Coefficient of Thermal Expansion/Contraction) to calculate the mixture CTEC or can directly input the mixture CTEC if known. Finally, the user inputs the 100 sec. or the 1000 sec. creep test data at high, intermediate and low temperatures (Fig. 7). The tool fits the creep compliance data with a Prony series model to characterize the mixture creep behavior in the form required by Illi-TC. A simplified 1D analysis is done by a preanalyzer module in the tool to identify the critical cooling events to minimize the time for FE analysis. The critical cooling events are identified as those events of thermal stresses that will exceed 80% of the tensile strength of the asphalt mixture. The program then performs a detailed FE analysis on the critical cooling events to determine the crack length, softening damage, and amount of predicted thermal cracking [12].

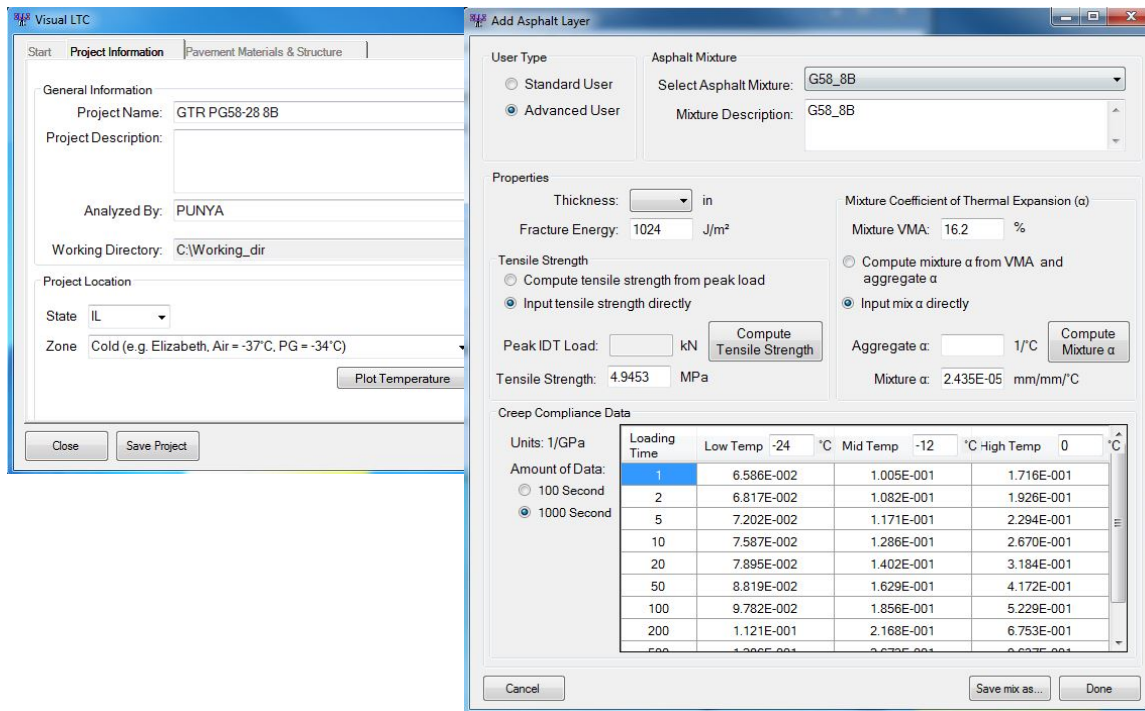


Figure 7. Illi-TC data input

## 4. RESULTS AND DISCUSSIONS

In the following sections, the DC(T) fracture energies along with the Hamburg rutting results are presented. Further, using the DC(T) and Hamburg results, Performance-Space plots are assembled and discussed.

### 4.1. Disk-Shaped Compact Tension Test

Fracture energy values of the nine mixes at -12°C and at -18°C for both field cores and gyratory samples were calculated. Three replicates of each mix were tested. Table 3 provides a summary of the results obtained.

Table 3. Summary of DC(T) Fracture Energy Results

	Plant-compacted gyratory samples				Field Cores			
	DC(T) $\Delta G_f$ @ T=-12°C	COV %	DC(T) $\Delta G_f$ @ T=-18°C	COV %	DC(T) $\Delta G_f$ @ T=-12°C	COV %	DC(T) $\Delta G_f$ @ T=-18°C	COV %
<b>GTR PG58-28</b>	1466	25%	895	15%	785	11%	664	6%
<b>GTR PG46-34</b>	2395	21%	1554	14%	2073	19%	1160	23%
<b>GTR PG46-34 High ABR</b>	1130	15%	1085	16%	1245	19%	865	2%
<b>Elastiko PG58-28</b>	901	9%	903	11%	785	10%	673	9%
<b>Elastiko PG46-34</b>	1108	3%	926	16%	980	19%	862	26%
<b>Elastiko PG46-34 High ABR</b>	903	19%	691	4%	905	17%	847	22%
<b>Evoflex PG58-28</b>	885	23%	771	25%	738	6%	803	21%
<b>Evoflex PG46-34</b>	944	16%	708	19%	1001	10%	906	17%
<b>Evoflex PG46-34 High ABR</b>	688	7%	842	18%	779	16%	700	18%

The UIUC research team determined that for the plant-produced gyratory samples, all specimens pass the recommended criteria of 690 J/m<sup>2</sup> for high-traffic volume road except Evoflex PG46-34 with high ABR, with a slightly failing value of 688 J/m<sup>2</sup> (Fig. 8). Fig. 8 shows the fracture energy of the mixes grouped as listed in the mixture matrix given in Table 1 for -12°C and -18°C. For -12°C, replacement with a softer binder in the mix bumps the fracture energy, and further addition of higher recycled asphalt in softer binder causes a drop in the fracture energy back to the approximate original test values for the first mix in each test group (the one containing PG XX-28 and lower ABR).

All the mixes, except two, show a decrease in the fracture energy at -18°C. The two exceptions are Elastiko PG58-28 mix wherein the difference in the fracture energies at the two temperatures is marginal, and Evoflex PG46-34 with high ABR wherein the difference is large. In general, the effect of high recycled asphalt on samples tested at -18°C is similar to the trend seen at -12°C; replacement with softer binder increases fracture energy and addition of recycled asphalt in softer binder brings the fracture energy back down to the range of the PG XX-28 mixtures with lower recycling. However, the Evoflex system did not follow this trend at -18°C in the case of the plant-produced specimens.

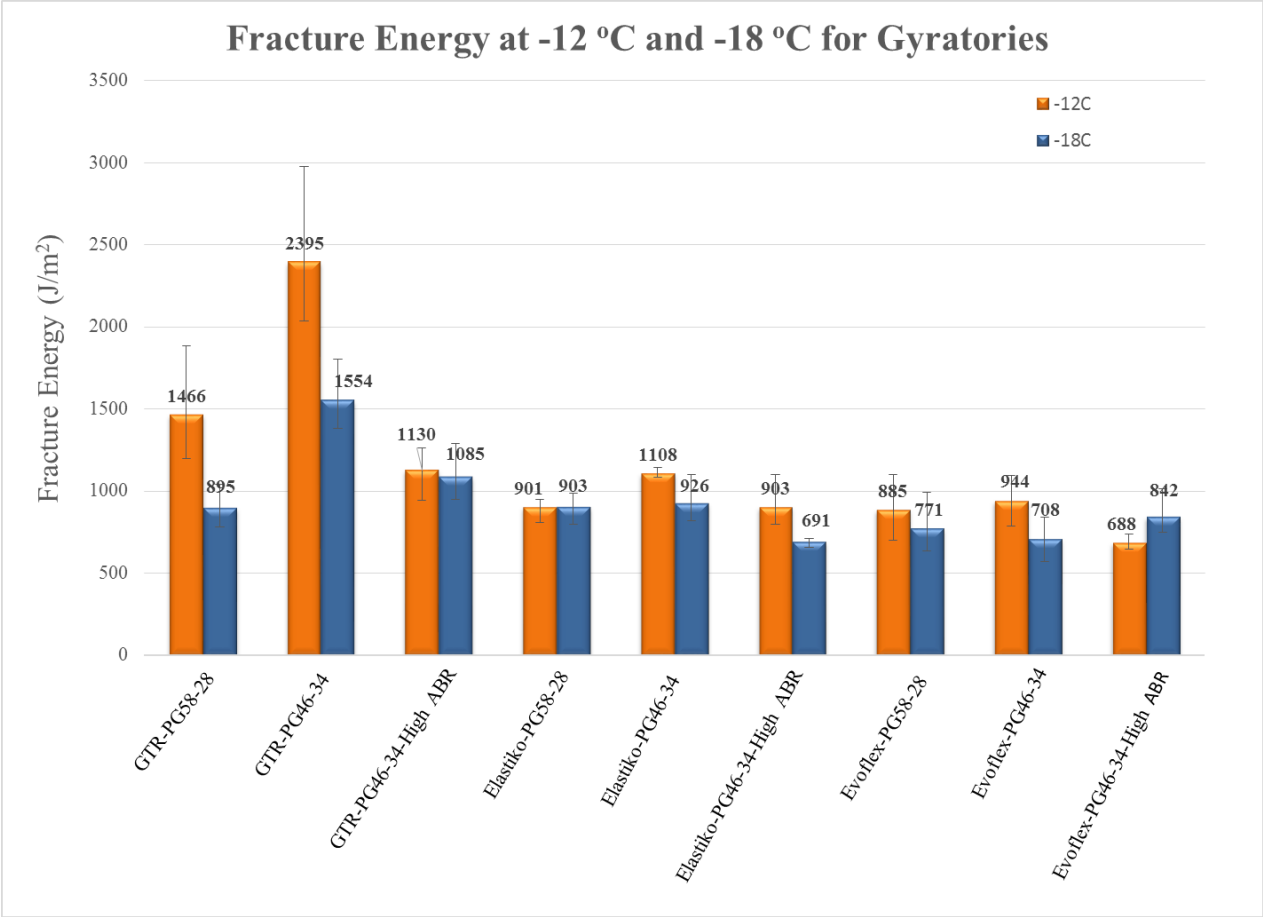


Figure 8. Fracture energies for plant-produced gytratory samples



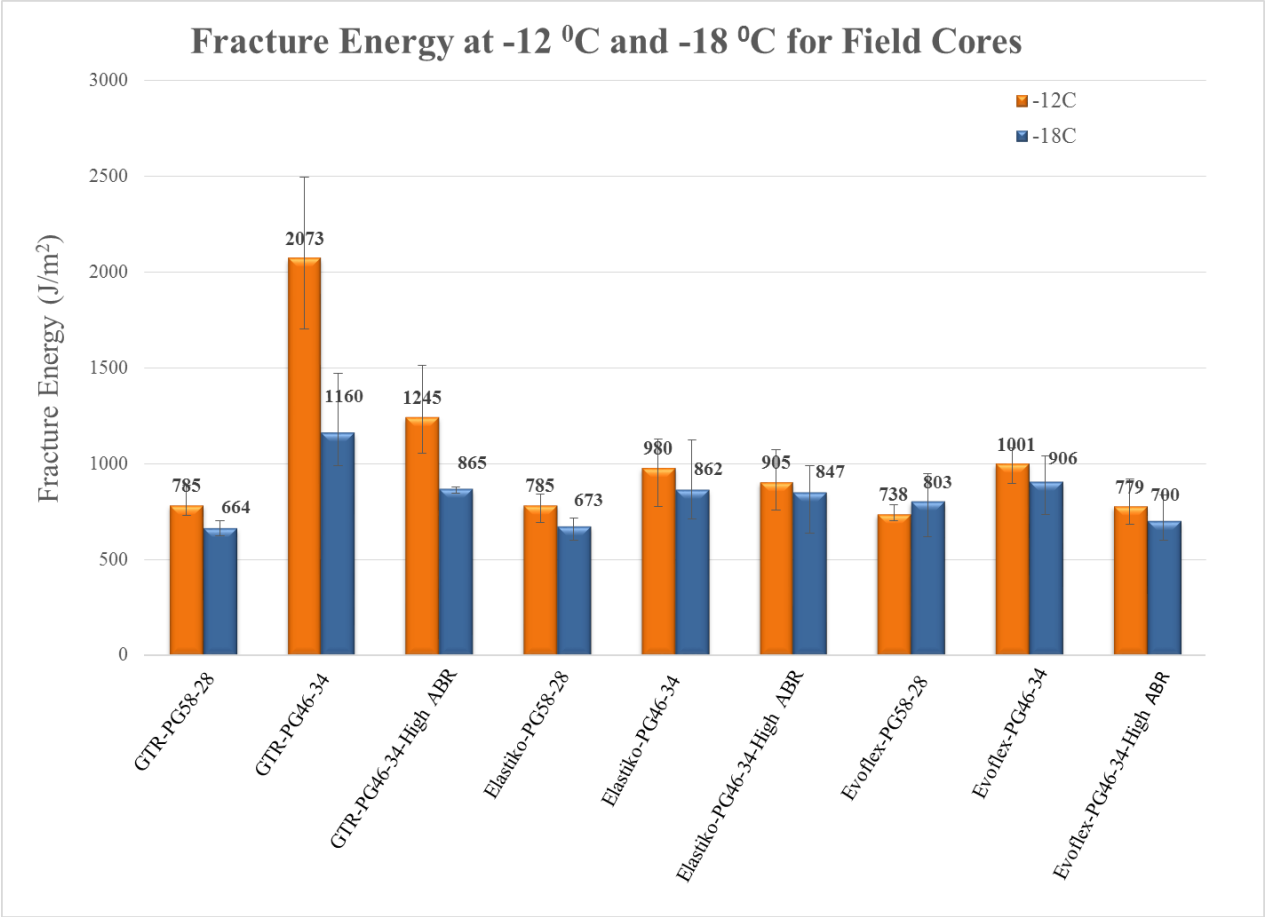


Figure 9. Fracture energies for field cores

Fig. 9 shows the fracture energy results obtained from the field cores at the two test temperatures. This trend also shows a bump in fracture energy with the addition of the softer binder, followed by a decrease in the value when the mix has a softer binder but also higher ABR for all the mix systems. All field cores pass the stringent criteria of 690 J/m<sup>2</sup> fracture energy at -12°C indicating a high resistance to thermal cracking. At -18°C, all the field cores are within 5% of passing the 690 J/m<sup>2</sup> criteria, which suggests that most of these mixtures would also be judged as highly thermal crack resistant even if the strict LTPP 98% reliability low temperature grade was used to set the DC(T) test temperature. The DC(T) results also point to the possibility of using high recycled asphalt content with these mix designs in conjunction with a softer binder without compromising fracture energy.

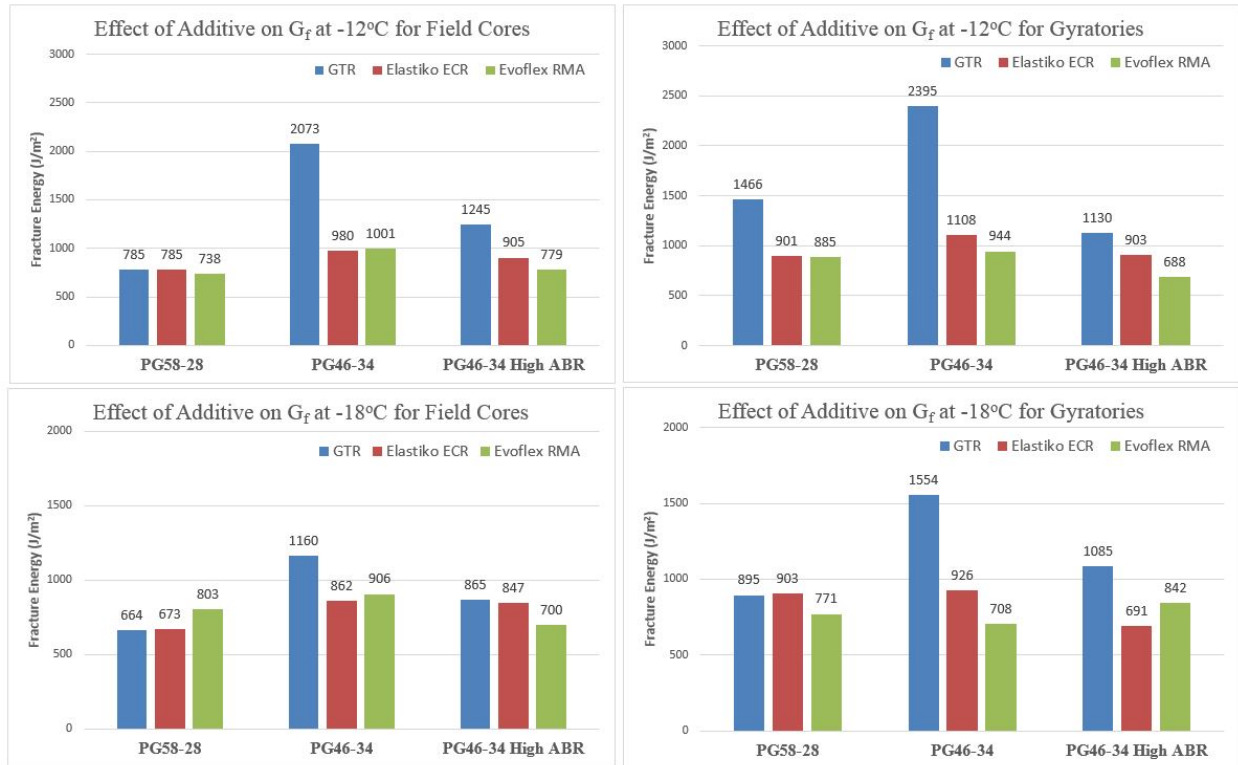


Figure 10. Effect of additives on fracture energy for particular binders

Fig.10 shows the effect of the additives by grouping the fracture energies with respect to different binder types. At  $-12^\circ\text{C}$ , GTR mixes have the highest fracture energy for all the binder types indicating higher potential in resisting low-temperature cracks. In the other two systems, Elastiko has better fracture energy in all cases except one, where the difference is not very high. For  $-18^\circ\text{C}$ , it is difficult to gauge which system would have better performance regarding fracture energy only.



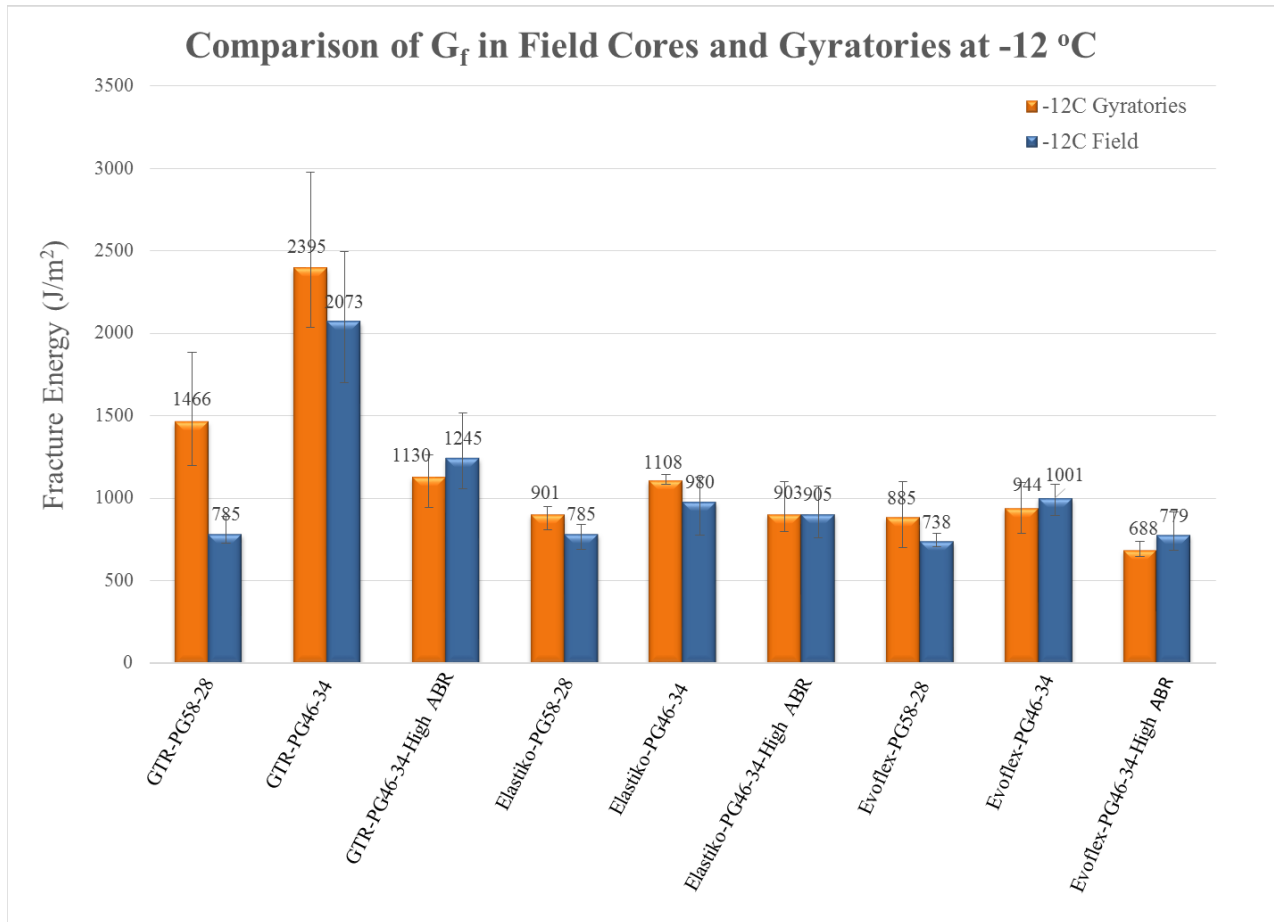


Figure 11. Comparison of fracture energies for field cores and plant-compacted gyratory samples for -12°C

Fig.11 provides a comparison of the fracture energy for field cores and the gyratory samples for the nine mixes, both tested at -12°C. All the mixes are fairly in close proximity of each other except the GTR system with base binder. This could be a result of various factors related to the field like varying level of compaction, different binder content in the field mix, mix gradation, etc. Fig.12 shows the comparison of the fracture energies for field cores and gyratory samples at -18°C, where the terminal-blend system again exhibits the highest fracture energy values.

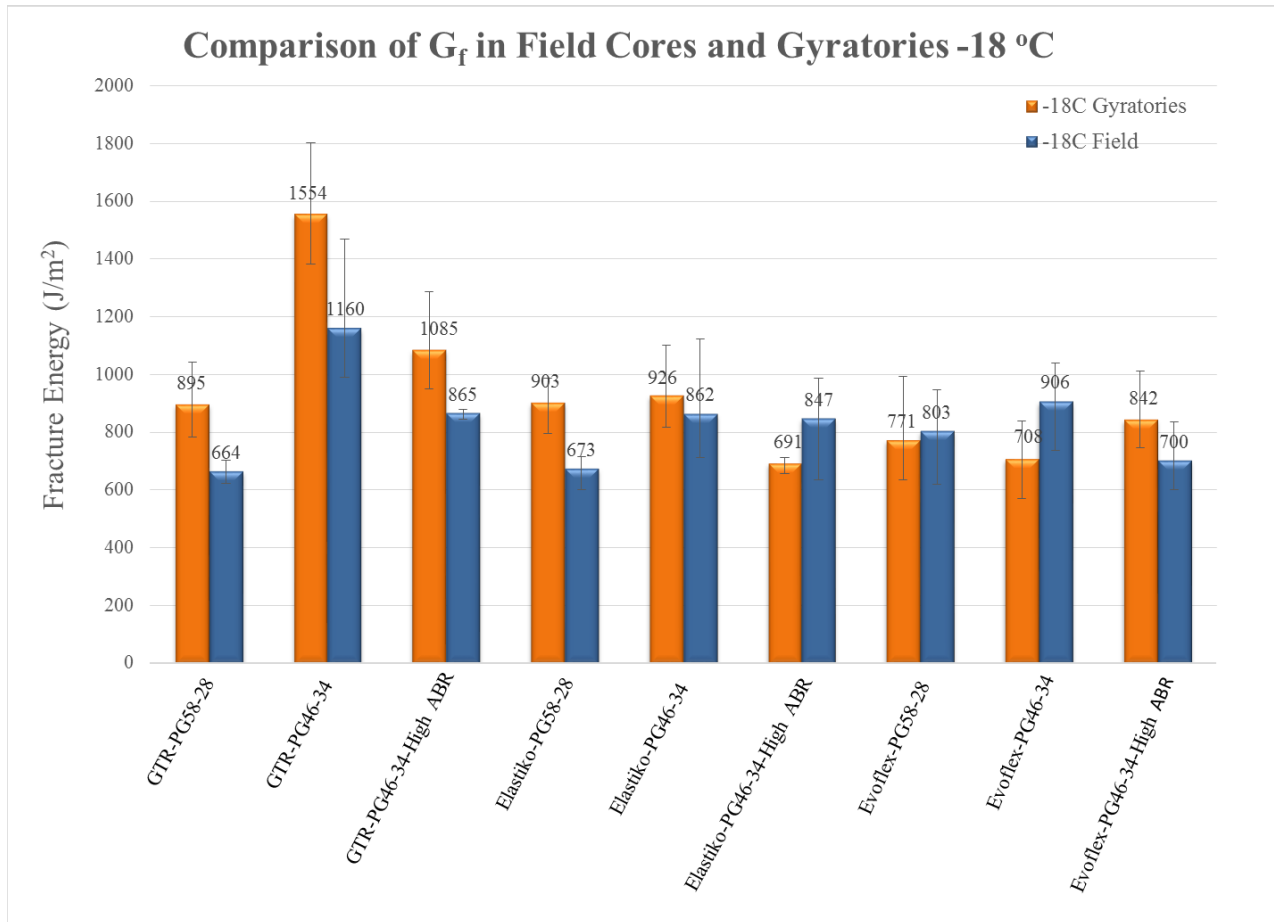


Figure 12. Comparison of fracture energies for field cores and plant-compacted gyratory samples for -18°C

#### 4.2. Hamburg Test Results

The Hamburg Wheel Tracking results provided by S.T.A.T.E. Testing are plotted in Fig. 13. As seen from the plot, all the mixes show a rut depth less than 6.0 mm at 20,000 passes, indicating excellent rut resistance in all of the mixes. The trend in results was as expected: replacement with softer binder increased the rut depth and addition of recycled asphalt caused the rut depth to lessen. The GTR46-34 mix showed the highest rut depth in the Hamburg testing. This correlates well to the high fracture energy as seen in the previous section. The softer binder makes the mastic softer, resulting in an elongated post-peak tail in DC(T) fracture energy test and a higher rut depth in the Hamburg test.

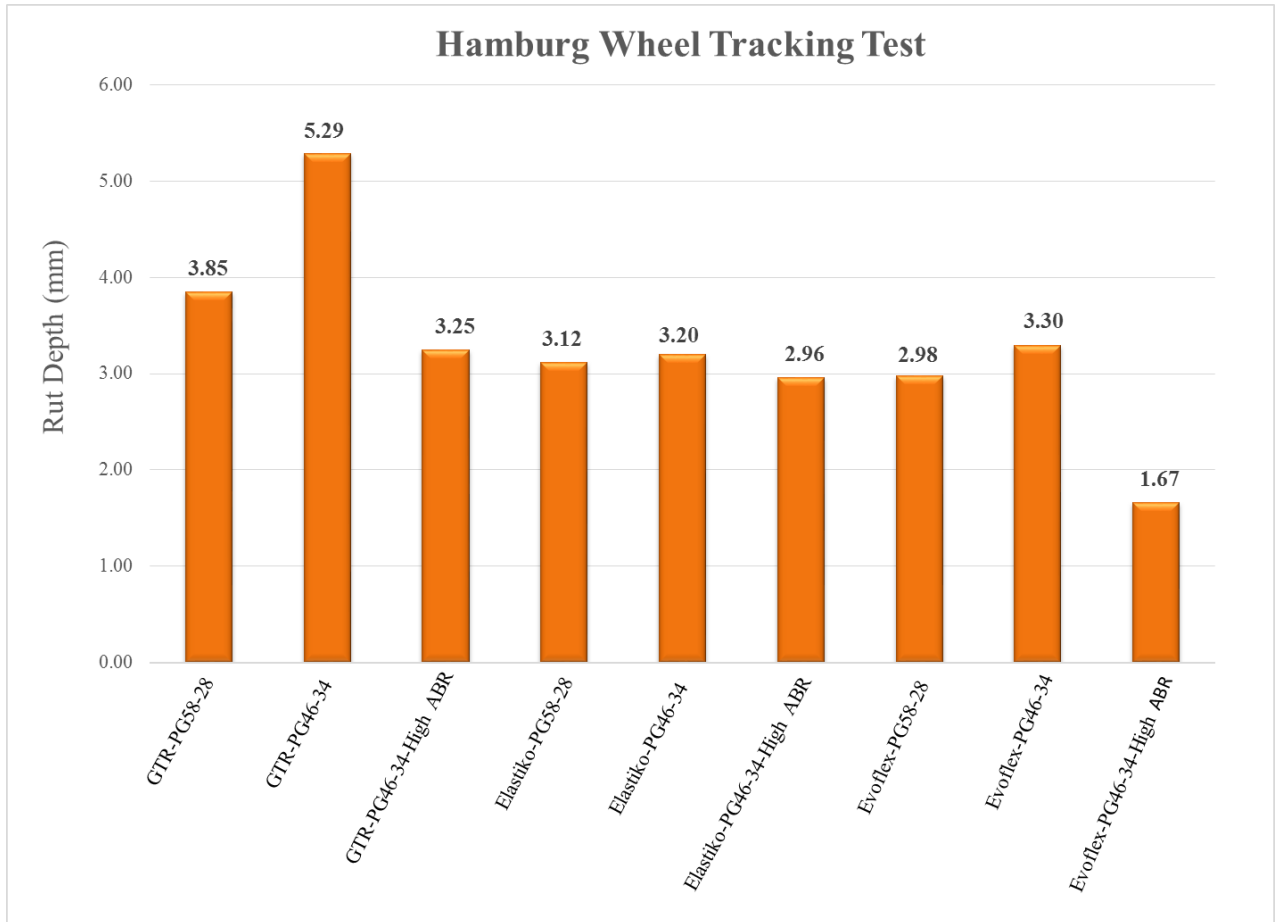


Figure 13. Hamburg Wheel Tracking Test

### 4.3. Performance-Space Diagram

As seen in Fig.14, all nine mixes fall in the upper-right section of the Hamburg-DC(T) plot, indicating good fracture energy and rut resistance. The Evoflex PG46-34 with high ABR mix falls on the borderline of the stringent criteria of  $690 \text{ J/m}^2$ . In the future, a softer binder could be used or less recycled asphalt may be added to increase the fracture energy of this particular mixture, since there is plenty of 'headroom' in the Hamburg result (low rut depth).

The arrows in the diagram show the shift of the mix on the plot with the substitution of a softer binder, and with the move to a higher percentage of recycled asphalt along with the softer (PGXX-34) binder. The shift stays within the confines of the right-upper section, indicating that a higher amount of RAP/RAS could be utilized if a softer binder is used. This result is consistent with what was inferred from the results of fracture energy in Section 4.1. In addition, the alignment of the data on a relatively straight line demonstrates a key advantage in pairing the Hamburg with the DC(T) as bookend performance tests; namely, that mix designers can use this relationship to expedite mix design by only running one of the tests during design iterations. It also suggests that the 3 GTR systems could likely be aligned on the performance-space diagram with proper choice of base (virgin) binder. For instance, the Elastiko product could be shifted either to the right (to coincide with the terminal-blend product) or to the left (to coincide with the RMA product) with the use of a softer or harder base binder, respectively. Following previous studies, the reason that the products fall on a line is that the mixes have similar aggregate type, aggregate structure and volumetrics. The main variable is the binder (or more correctly, mastic) rheological and fracture properties. This indirectly suggests that the combinations of virgin and recycled binder, rubber, and polymer (in the case of the RMA product) in these mixtures

differ, but have similar contribution to the overall mix performance and can likely be shifted around with choice of base binder (or by using other stiffening or softening additives).

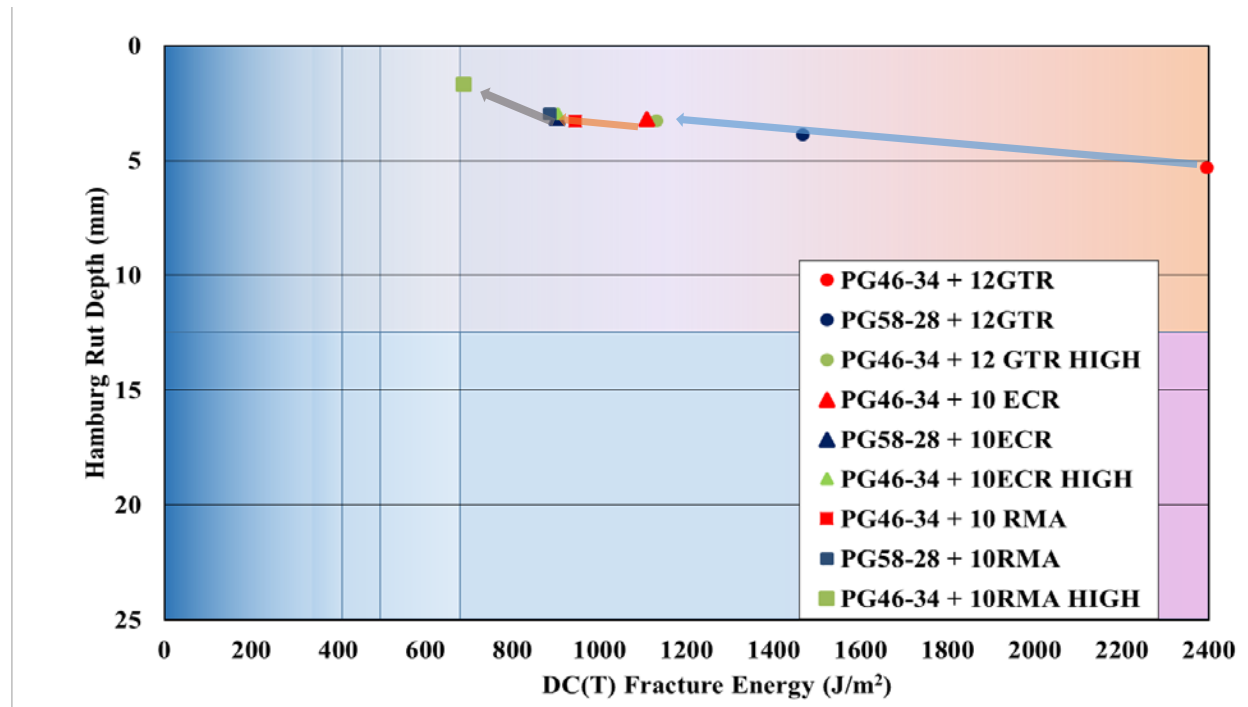


Figure 14. Performance-Space Diagram

#### 4.4. Illi-TC Results

The creep and fracture data for all the mixes were used in the Illi-TC model to predict the thermal cracking potential of the mixes in the field. Illi-TC has statewide built-in temperature profiles, and it divides those profiles into cold, intermediate, and warm climates. The cold climate option for Illinois, which is the temperature profile of Elizabeth Illinois, was used in the modeling as it was deemed the closest available location found in the software relative to the demonstration project location. The IDT tensile strength was computed using the DC(T) peak load, and the creep compliance results from three test temperatures were input in the tool. A mixture CTEC value of  $2.435 \times 10^{-5}$  mm/mm/°C was used for all mixes. This value is a typical value used for Illinois mixes. Furthermore, the mixes mostly are made up of quartzite aggregates (CM-14), and the CTEC values of quartzite aggregates are reported to be  $1.08 \times 10^{-5}$  mm/mm/°C. Putting in this value along with the VMA, the mixture CTEC value is close to the value assumed in all the cases. Since the fracture test results after creep had shown some damage to the specimens, the creep test values for each mix was run using the fracture energy and peak load values from the DC(T) fracture energy test only (without creep). The least possible thickness option in the software was taken during the analysis to simulate a worst-case scenario in terms of temperature-induced stress. As shown in Table 4 for plant-compacted gyratory samples and in Table 5 for field cores, all the mixtures had no critical events, which indicates that no transverse cracking in the pavement surfaces are expected to occur due to thermal stresses. The computed thermal stresses were very low in all cases, which could be due to the high fracture energy and peak load values of all mixtures, along with reasonably high creep compliance values due to proper mix design and material selection approaches. This demonstrates that the creep and fracture characteristics of all nine mixes were in balance with respect to thermal cracking resistance. In other words, the thermal stresses expected to develop based on the low-temperature mix rheology (creep compliance) is well under the fracture threshold of the mixes.

Table 4 . Critical Events count from Illi-TC runs for plant-compacted gyratory samples

	PG of Binder	Fracture Energy ( $G_f$ )	Peak Load	Calculated Tensile Strength	Critical Events
		J/m <sup>2</sup>	kN	MPa	#
	PG58-28	1466	3.5	5.1	0
	PG46-34	2395	3.4	4.9	0
	PG46-34 High ABR	1130	4.1	5.9	0
	PG58-28	901	3.3	4.8	0
	PG46-34	1108	3.9	5.7	0
	PG46-34 High ABR	903	3.9	5.7	0
	PG58-28	885	3.3	4.8	0
	PG46-34	944	3.7	5.4	0
	PG46-34 High ABR	688	3.4	4.9	0

Table 5. Critical Events count from Illi-TC runs for field cores

	PG of Binder	Fracture Energy ( $G_f$ )	Peak Load	Calculated Tensile Strength	Critical Events
		J/m <sup>2</sup>	kN	MPa	#
	PG58-28	805	3.6	5.2	0
	PG46-34	1074	3.1	4.5	0
	PG46-34 High ABR	820	3.2	4.7	0
	PG58-28	793	3.0	4.4	0
	PG46-34	833	3.0	4.4	0
	PG46-34 High ABR	699	3.5	5.1	0
	PG58-28	630	3.0	4.4	0
	PG46-34	767	3.3	4.8	0
	PG46-34 High ABR	745	3.1	4.5	0

#### 4.5. Acoustic Emission Test Results

The acoustic emission (AE) testing, detailed in Appendix-B, largely agreed with fracture energy findings in regards to the relative trends in fracture energy found in the DC(T). The use of a softer base binder generally decreased the embrittlement temperature, and the addition of recycled asphalt shifted it back to a warmer embrittlement temperature. The terminal blend product exhibited the best low temperature cracking performance, especially in the field core set. The field core embrittlement temperatures were in general lower than the lab-compacted specimens, possibly

indicating differences in short-term aging between the two data sets, which affected measurable acoustic emission activities. The repeatability of the AE test is generally quite good, which was indeed found to be the case here (a number of single-digit COV values were computed).

## 5. CONCLUDING REMARKS

In Phase-I of the project, field cores and plant-produced gyratory samples were tested in the DC(T) machine to ascertain their fracture energies at two test temperatures,  $-12^{\circ}\text{C}$  and  $-18^{\circ}\text{C}$ . Typically,  $-12^{\circ}\text{C}$  is the DC(T) test temperature used for the Illinois climate. For  $-12^{\circ}\text{C}$ , considering both the field cores and the plant-produced gyratory samples, only one mixture failed to satisfy the stringent criteria of  $690 \text{ J/m}^2$ , recommended by Marasteanu, et al. [13]. All mixes were found to pass the stringent Tollway Hamburg criteria. At  $-18^{\circ}\text{C}$ , the fracture energies drop from that at  $-12^{\circ}\text{C}$  in most of the cases. However, only two field cores did not satisfy the strict criteria of  $690 \text{ J/m}^2$  and were in fact within a 5% margin of passing even at this more severe test condition.

The DC(T) results of the mixes with a softer binder and softer binder combined with high ABR sheds light on the feasibility of using more recycled materials in conjunction with a softer binder. Given the importance pavement recycling in transportation sustainability, mixes with a higher percentage of recycled material lying on the upper-right section of the performance-space diagram represents a very favorable scenario. In addition, the alignment of the data on a relatively straight line demonstrates the advantage of pairing the Hamburg with the DC(T) as bookend performance tests; namely, that mix designers can use this relationship to expedite mix design by only running one of the tests during design iterations. Or stated otherwise, that any given mixture change would have predictable effects on both Hamburg and DC(T) test results. It also suggests that the three systems could likely be aligned on the performance-space diagram with proper choice of base (virgin) binder; i.e., that the swollen GTR in each of these systems behave in a similar fashion, while that the rheological behavior of their as-produced binder/mastic systems vary.

A new creep compliance procedure was developed using the DC(T) device as an alternative to the traditional IDT test (AASHTO T-322). The temperature shift factors were graphically determined, creep compliance master curves were constructed, and a generalized Voigt-Kelvin model was fit for each mix at a reference temperature of  $-24^{\circ}\text{C}$ . The DC(T) master curves were found to be smooth with good overlap and followed the expected relative rankings based on DC(T) testing, binder grade and recycled material content. DC(T) fracture tests were also performed on the specimens after the completion of creep compliance testing. The fracture energies calculated for the specimens after they underwent creep tests at three temperatures using the new protocol were lower than the fracture energy values for the same mix systems obtained without any prior creep compliance testing. Based on these findings, a revised DC(T) creep test protocol will be created with longer relaxation periods between creep tests, and with lower creep loads. This will allow a single specimen to be used for each creep and fracture test replicate, rather than doubling the number of specimens needed to conduct both tests.

Illi-TC modeling demonstrated that all nine mixes should be thermal-crack-free throughout their design lives. Overall, the 3 GTR systems and 9 mixes investigated look very promising as far as low-temperature cracking and rutting are considered. All mixtures had high fracture energy, good creep/relaxation characteristics, zero thermal cracking potential, and excellent rutting resistance. Construction, economic, and environmental factors should be evaluated in a future study to further characterize these and other related GTR technologies to aid in future designs and specification advances. Also, performance testing standards for mix design and for quality control (and possibly acceptance) should be formalized for the various mix types used by the Illinois Tollway.

## 6. REFERENCES

- [1] M. A. Heitzman, "State of the Practice- Design and construction of asphalt paving materials with crumb rubber modifier," 1992.
- [2] State of California Department of Transportation, "Use of scrap tire rubber - State of the technology and best practices" 2005.
- [3] B. Bairgi, Z. Hossain, and R. D. Hendrix, "Investigation of rheological properties of asphalt rubber toward sustainable use of scrap tires," *Int. Found. Congr. Equip. Expo 2015, IFCEE 2015*, vol. GSP 256, pp. 359–368, 2015.
- [4] J. Richard Willis, "Effect of Ground Tire Rubber Particle Size and Grinding Method on Asphalt Binder Properties," *NCAT Rep. 12-09*, no. October, 2012.
- [5] O. Xu, L. Cong, F. Xiao, and S. N. Amirkhanian, "Rheology investigation of combined binders from various polymers with GTR under a short term aging process," *Constr. Build. Mater.*, vol. 93, pp. 1012–1021, 2015.
- [6] S. Vahidi, W. S. Mogawer, and A. Booshehrian, "Effects of GTR and Treated GTR on Asphalt Binder and High-RAP Mixtures Materials," vol. 26, no. April, pp. 721–727, 2014.
- [7] R. C. Williams, E. Joana, J. Ferreira, and F. Peralta, *Development of Non-Petroleum-Based Binders for Use in Flexible Pavements – Phase II Development of Non-Petroleum- Based Binders for Use in Flexible Pavements – Phase II Final Report*. 2015.
- [8] C. K. Akisetty, S. Lee, and S. N. Amirkhanian, "High temperature properties of rubberized binders containing warm asphalt additives," *Constr. Build. Mater.*, vol. 23, no. 1, pp. 565–573, 2009.
- [9] C. Te Chiu and L. C. Lu, "A laboratory study on stone matrix asphalt using ground tire rubber," *Constr. Build. Mater.*, vol. 21, no. 5, pp. 1027–1033, 2007.
- [10] ASTM, "Standard Test Method for Determining Fracture Energy of Asphalt-Aggregate Mixtures Using the Disk-Shaped Compact Tension Geometry," *ASTM Int. Stand.*, pp. 2–8, 2013.
- [11] W. G. Buttlar, B. C. Hill, H. Wang, and W. Mogawer, "Performance space diagram for the evaluation of high- and low-temperature asphalt mixture performance," *Road Mater. Pavement Des.*, vol. 0, no. 0, pp. 1–23, 2016.
- [12] E. V. Dave, W. G. Buttlar, S. E. Leon, B. Behnia, and G. H. Paulino, "IlliTc-Low temperature cracking model for asphalt pavements," *Asph. Paving Technol. Assoc. Asph. Paving Technol. Tech. Sess.*, vol. 82, no. January 2014, pp. 91–126, 2013.
- [13] M. O. Marasteanu, W. G. Buttlar, H. Bahia, C. R. Williams, and E. Al., "Investigation of Low Temperature Cracking in Asphalt Pavements Phase-II," no. May, pp. 1–4, 2012.
- [14] R. Roque and W. G. Buttlar, "The development of a measurement and analysis system to accurately determine asphalt concrete properties using the indirect tensile mode (with discussion)," *J. Assoc. Asph. Paving Technol.*, vol. 61, 1992.
- [15] E. V. Dave, B. Behnia, S. Ahmed, W. G. Buttlar, and H. Reis, "Low Temperature Fracture Evaluation of Asphalt Mixtures Using Mechanical Testing and Acoustic Emission Techniques," 2013, pp. 193–225.
- [16] W. G. Buttlar, B. Behnia, and H. M. Reis, "An Acoustic Emission-Based Test to Determine Asphalt Binder and Mixture Embrittlement Temperature," no. November, 2011.
- [17] B. Behnia, E. V. Dave, S. Ahmed, W. G. Buttlar, and H. Reis, "Effects of Recycled Asphalt Pavement Amounts on Low-Temperature Cracking Performance of Asphalt Mixtures Using Acoustic Emissions," *Transp. Res. Rec. J. Transp. Res. Board*, vol. 2208, no. 1, pp. 64–71, 2011.

- [18] B. Behnia, "An Acoustic Emission-based Test to Evaluate Low Temperature Behavior of Asphalt Materials," 2013.



## Appendix A: DC(T) Creep Compliance

The creep compliance of asphalt mixtures, when combined with the fracture energy values, complete the parametric requirements to study thermal cracking effectively. An asphalt mixture's resistance to cracking not only depends on its fracture energy, but also on its ability to relax thermal stresses as they develop during a cooling cycle.

Traditionally, creep compliance of asphalt mixtures is measured by indirect tensile (IDT) creep test that is described in the AASHTO T 322 standard. The IDT creep test was developed by Roque and Buttlar (1992) in the early 1990s as part of SHRP A-357 project at Penn State University [14]. The test utilizes a cylindrical sample of 150 mm diameter and 50 mm height. The sample is loaded vertically along the diameter of the specimen. Extensometers are attached to each flat face of the specimen at roughly its center that measure the horizontal and vertical strains in the specimen due to the vertical load. The load level is adjusted such that the response of the specimen falls within the linear viscoelastic range.

Kebede (2012) proposed a new method that combined creep compliance testing with the DC(T) fracture energy test. He conducted creep compliance tests with DC(T) specimen geometry; each specimen mounted only with an extensometer near the crack tip. After the creep compliance tests at static loads were done, the specimen was subjected to the usual DC(T) fracture energy test. Since creep testing generally operates within the linear viscoelastic range of stresses and strains, the specimen undergoing creep tests are expected to recover fully before the fracture energy test is started. Kebede performed 2-D elastic simulations of the DC(T) creep test to select the location of the horizontal extensometer and to evaluate the possibility of formation of micro-cracks during the creep test, which would presumably affect the fracture energy results.

Encouraged by favorable results from the above study, a DC(T) creep test measuring horizontal displacements with the Crack Mouth Opening Displacement (CMOD) measurement instead of an extensometer was developed as a part of this project. The main aim of developing this test is to reduce the time, effort, and cost to obtain creep test results in future studies. Kebede pointed out that DC(T) creep with CMOD reduced the time taken for the test in almost half in comparison to IDT creep test. In addition, the new test with CMOD measurements requires no fabrication to attach an extensometer and no add-ons to the DC(T) machine to obtain horizontal strain data. In his thesis, Kebede showed through simulations that the location of the extensometer should be 10 mm away from the notch tip because the stress distributions were uniform at that part of the sample. However, it can be argued that appropriate correction factors can compensate for the horizontal displacement measurement at the crack mouth opening. Presently, an attempt has been made to compute creep compliance by using only the existing CMOD clip gauge to measure the viscoelastic tensile response to load.

### DC(T) Creep Compliance Testing Results

The DC(T) creep compliance tests were carried out at 0°C, -24°C, and -12°C, in that particular order. DC(T) fracture tests were done immediately after the -12°C DC(T) creep tests. AASHTO T322 was followed to decide the DC(T) creep compliance test protocol. All the samples were temperature conditioned for 3±1 hours in the DC(T) chamber at the test temperature before starting the test. The specimens were then mounted on the loading pins and a seating load of 0.1kN was applied. The test runs on a static loading condition and the total load applied is the seating load plus the creep load. Once the test is complete, the software outputs the creep compliance values calculated using the following formula:

$$D(t) = \frac{C * d(t) * T}{P}$$

C = Correction factor

d(t) = Adjusted CMOD at time t sec., in mm.

T = thickness of the specimen, in mm.

P = applied load, in kN

As shown above, a correction factor is needed to account for the geometry effect of the disk-shaped specimen on the creep compliance results. Therefore, a 2-D elastic DC(T) model was built in the commercially available FEM software, ABAQUS, to determine the correction factor of DC(T) creep compliance results (shown in Fig. 19). As the material is still within linear stress-strain range in the first 30 seconds of the creep compliance test, the elastic assumption will be appropriate to take in the model. In this way, the correction factor can be predicted based the proportional relationship between the load and deflection of the specimen. In the finite element model, the material was assumed to be elastic, homogeneous and isotropic, Poisson's ratio and elastic modulus were assumed to be 0.35 and 1000 MPa, accordingly, and 1 kN was applied at each side of the loading hole. The correction factor was calculated to be 0.075.

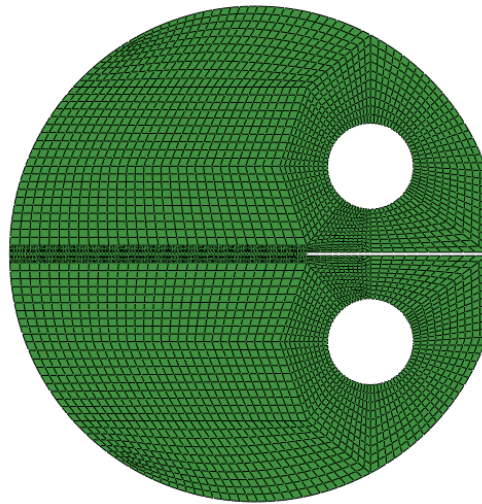


Figure 15. 2-D elastic model to simulate DC(T) Creep

The creep load for this initial round of DC(T) creep testing was set at 0.9 kN for 0°C and 1 kN for -12°C and -24°C. The loads were estimated with the goal that the specimens would not undergo any damage due to deformation and at the same time they would deform enough for the response to be picked up by the clip gage. Fortunately, the peak loads of the mix types were known before-hand, which helped in roughly estimating the creep load. A more robust method of choosing creep load, based on the CMOD response in the initial loading period, is being devised through FEM and its validation in ongoing work. In retrospect, we found that our load levels were too high, perhaps as much as double the range required to limit damage to insignificant levels.

The six-parameter Voigt-Kelvin model was used to fit the master curves plotted using the time-temperature superposition principle with the reference temperature of 24°C. The creep compliance curves for the mixes are shown in Fig. 16-18. As shown in the figures, the creep compliance curves are smooth, and the trends are as expected. In all three types of products, the softer binder system (PG 46-34) has higher creep compliance values. The effects of high ABR content can be clearly seen in the creep compliance curves. The addition of more recycled content leads to a stiffer mix and consequently the creep compliance curve shifts downwards. A power-law model was also used to fit the master curves, and the m-values were calculated for the mixes. The values are shown in Table 6.

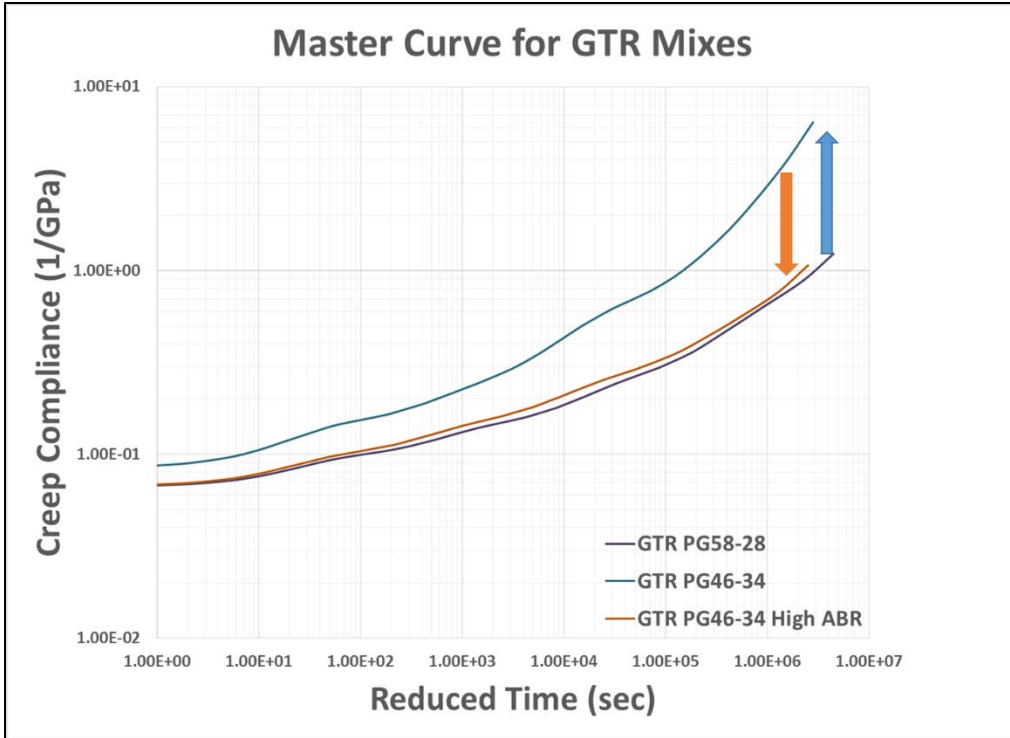


Figure 16. Master curve for GTR mixes (gyratory samples)

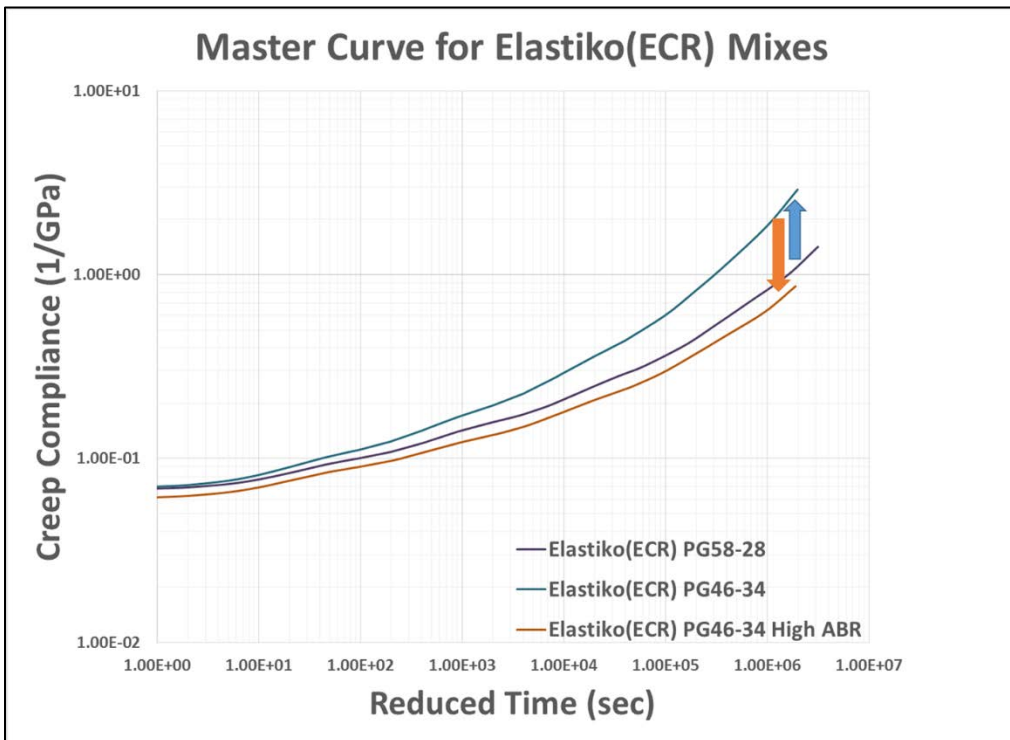


Figure 17. Master curve for Elastiko (ECR) mixes (gyratory samples)

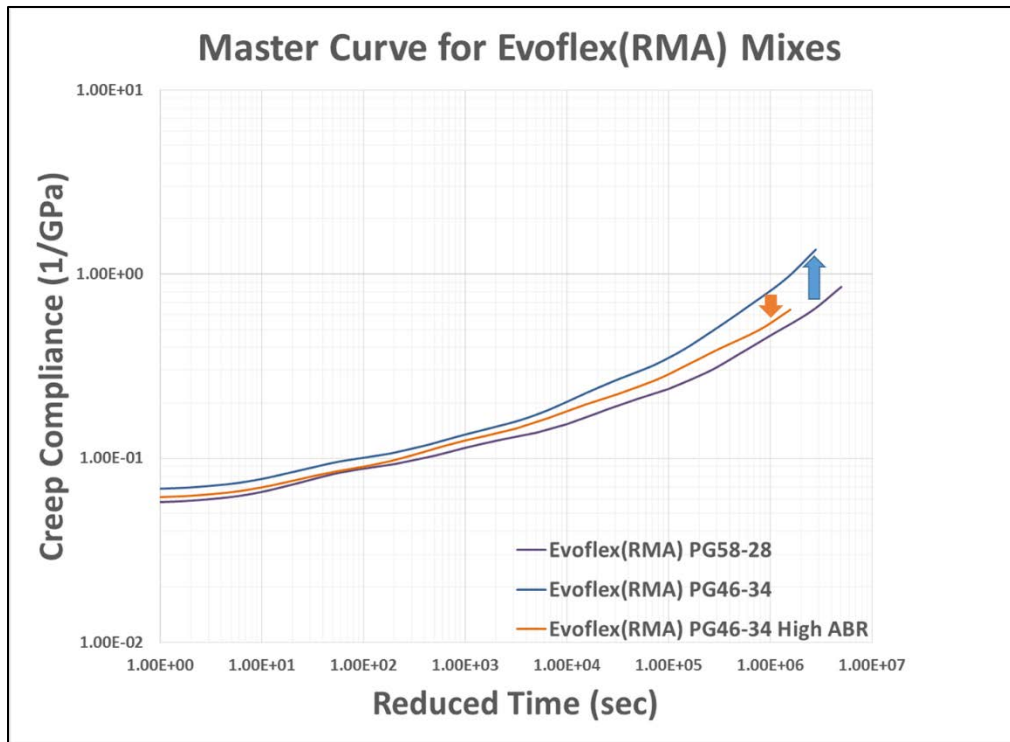
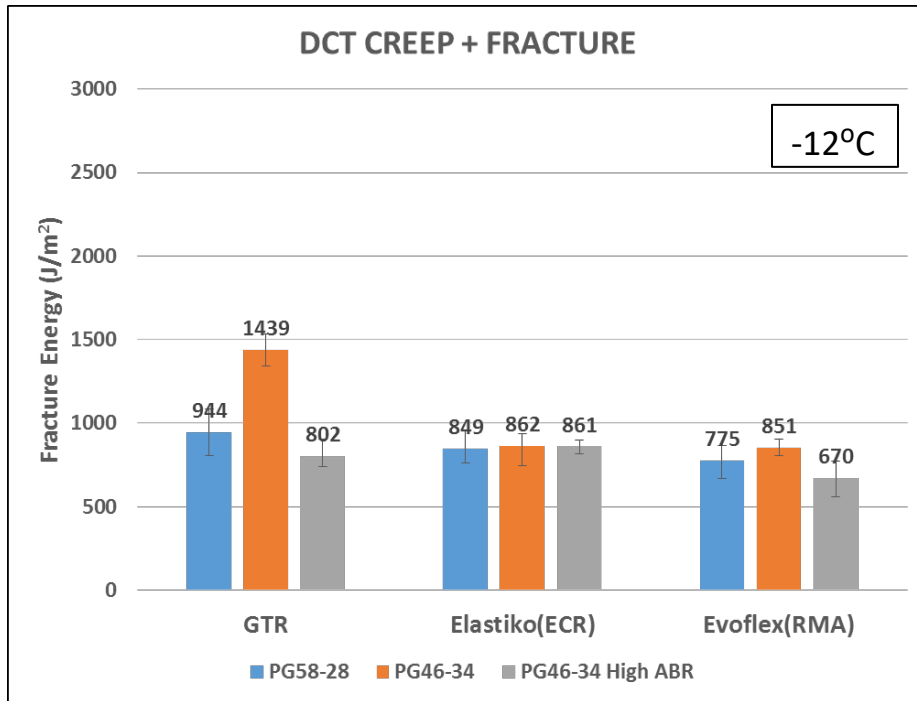


Figure 18. Master curve for Evoflex(RMA) mixes (gyratory samples)

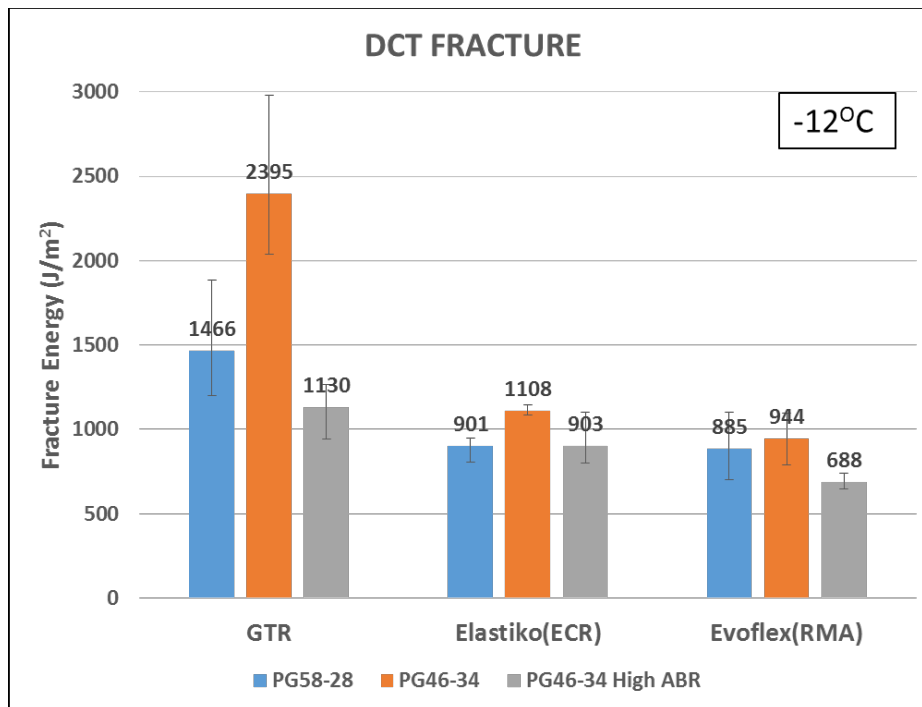
Table 6. m-value for plant-compacted gyratory samples

	<b>PG58-28</b>	<b>PG-46-34</b>	<b>PG46-34 High ABR</b>
<b>GTR</b>	0.430	0.707	0.403
<b>Elastiko (ECR)</b>	0.445	0.573	0.393
<b>Evoflex (RMA)</b>	0.384	0.460	0.325

Immediately after performing creep test at -12°C, the specimens were fractured at the same temperature. The fracture energy values obtained after creep testing have been shown in Fig. 19 (a), and the fracture energy values obtained without any creep testing have been shown in Fig. 19(b).



a



b

Figure 19. a) DC(T) fracture energy values after creep testing b) DC(T) fracture energy test results without any creep compliance testing (Test temperature = -12°C)

It can be seen from Fig 19 that the fracture energy values show familiar trends for all of the mixes. However, the fracture energy values are lower when the fracture energy test was done after the creep testing for the load levels used in this first attempt to develop a CMOD-based DC(T) creep test. This could also be due to the lack of relaxation time between the creep compliance and fracture energy testing at -12°C. The softest terminal-blend GTR mixes showed the maximum effect of the creep testing on their fracture energies. Table 7 shows the damage induced due to creep loads regarding percentage by comparing the fracture energies obtained in the two methods of testing. The Evoflex (RMA) and Elastiko (ECR) mixes did not show as much damage as compared to the terminal blend product, i.e., their fracture energy values after creep testing was more comparable to the fracture energy values on specimens without any creep testing. The higher deformation level measured in the terminal blend mixes seem to be associated with the higher levels of creep damage. This suggests that the maximum load level should be tied to mixture compliance; softer mixes should utilize lower loads in order to minimize damage during creep testing.

The present standard test to obtain creep compliance – Indirect Tensile Creep Compliance (AASHTO T-322) – limits the horizontal deformation to 0.00125 mm-0.0190 mm for 150 mm specimens. If either limit is violated then the standard recommends to stop the test, allow the specimen to recover for 5 minutes and restart the test with an adjusted load. In the future, the data in Table 7 can be used to come up with a similar load limit or a CMOD limit to prevent the creep load from inducing any damage in the specimen during the test.

Table 7. Damage percentages of plant-compacted gyratory mixes

	PG of Binder	DC(T) Creep+Fracture	DC(T) Fracture	Damage
		J/m <sup>2</sup> (A)	J/m <sup>2</sup> (B)	(%) ((B-A)/B)
	PG58-22	944	1466	36%
	PG46-34	1439	2395	40%
	PG46-34 High ABR	802	1130	29%
	PG58-22	849	901	6%
	PG46-34	862	1108	22%
	PG46-34 High ABR	861	903	5%
	PG58-22	775	885	12%
	PG46-34	851	944	10%
	PG46-34 High ABR	670	688	3%

A similar procedure for creep compliance testing was followed for the field cores. However, the creep load was changed based on the experience gathered from testing the gyratory samples, and also according to the thickness of the field core DC(T) specimen. Table 8 shows the load levels used in all the specimens. In general, 0.7 kN creep load was selected for samples tested at 0°C and 0.8 kN creep load was used at -12°C and -24°C. The load was scaled for thickness variation.

Table 8. Creep load levels for different field cores

<b>GTR</b>			
<b>Binder</b>	<b>Specimen #</b>	<b>Load at 0°C</b>	<b>Load at -12 °C and -24 °C</b>
	3	0.7	0.8
	8	0.7	0.8
	10	0.7	0.8
	13	0.7	0.8
	22	0.7	0.8
	-	-	-
	28	0.7	0.8
	33	0.9	0.8
	36	0.7	0.8
<b>ELASTIKO (ECR)</b>			
<b>Binder</b>	<b>Specimen #</b>	<b>Load at 0°C</b>	<b>Load at -12 °C and -24 °C</b>
	1	0.7	0.8
	3	0.7	0.8
	5	0.7	0.8
	20	0.6	0.8
	23	0.7	0.8
	24	0.7	0.8
	26	0.7	0.8
	27	0.7	0.8
	30	0.7	0.8
<b>EVOFLEX (RMA)</b>			
<b>Binder</b>	<b>Specimen #</b>	<b>Load at 0°C</b>	<b>Load at -12 °C and -24 °C</b>
	4	0.5	0.7
	8	0.6	0.8
	9	0.6	0.8
	15	0.6	0.8
	16	0.6	0.8
	21	0.7	0.8
	27	0.5	0.7
	33	0.6	0.8
	--	0.6	0.8

The creep compliance master curves are shown in Fig. 20-22. The trends seen were as expected and similar to the plant-compacted gyratory samples. All the mixture systems (GTR, ECR, and RMA) showed lower creep compliance with stiffer binder, higher creep compliance with softer binder, and became stiffer with addition of recycled material. The only exception to this was seen in Elastiko product with PG58-28 binder. The creep compliance master curves for base binder (PG58-28) and softer binder (PG46-34) were found to be very similar.

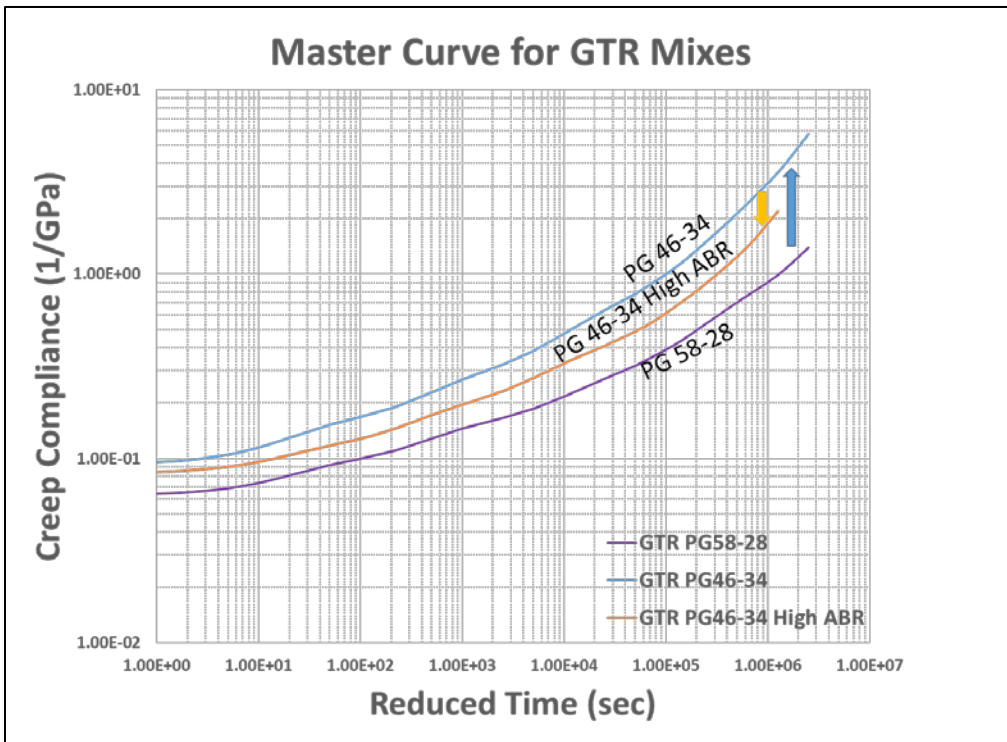


Figure 20. Creep compliance master curve for GTR field cores

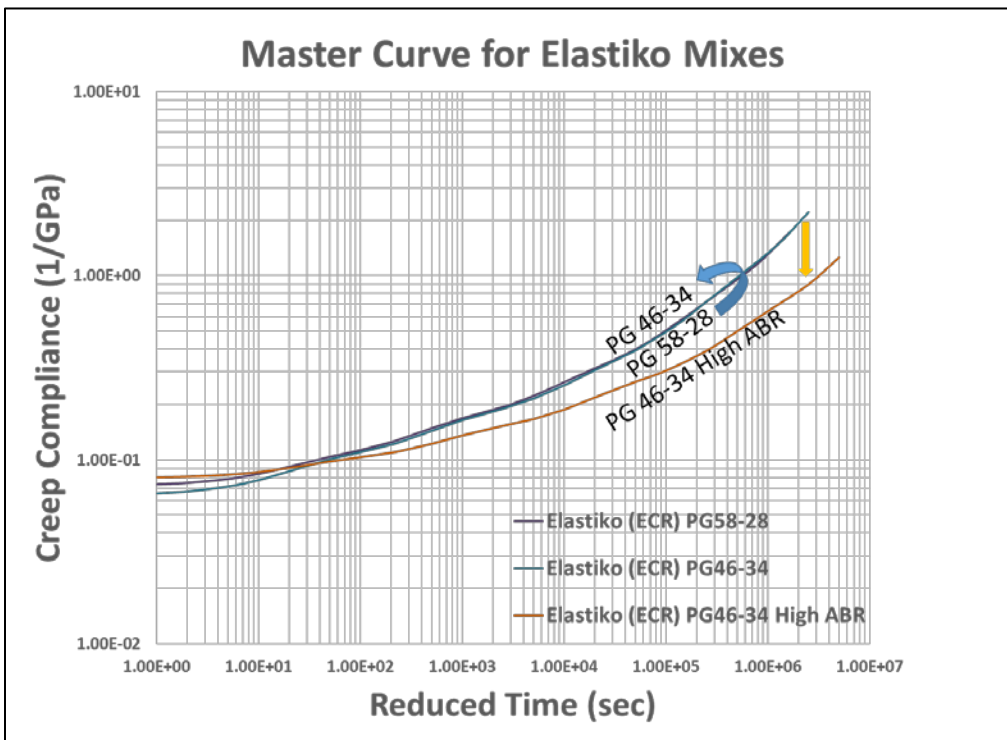


Figure 21. Creep compliance master curve for Elastiko (ECR) field cores



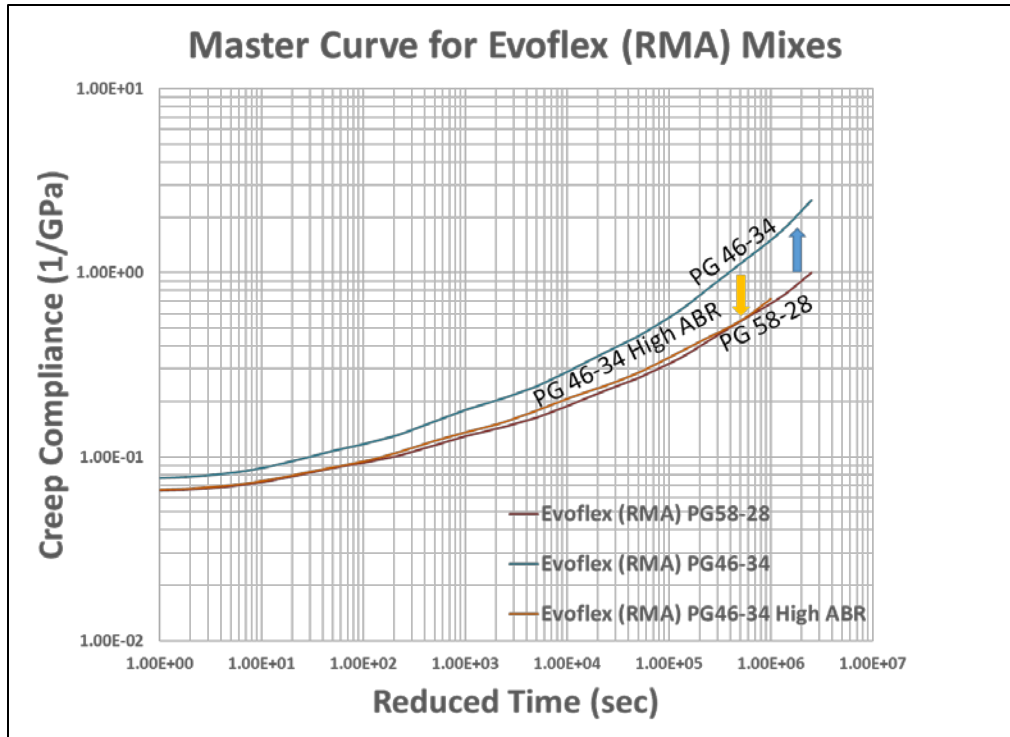


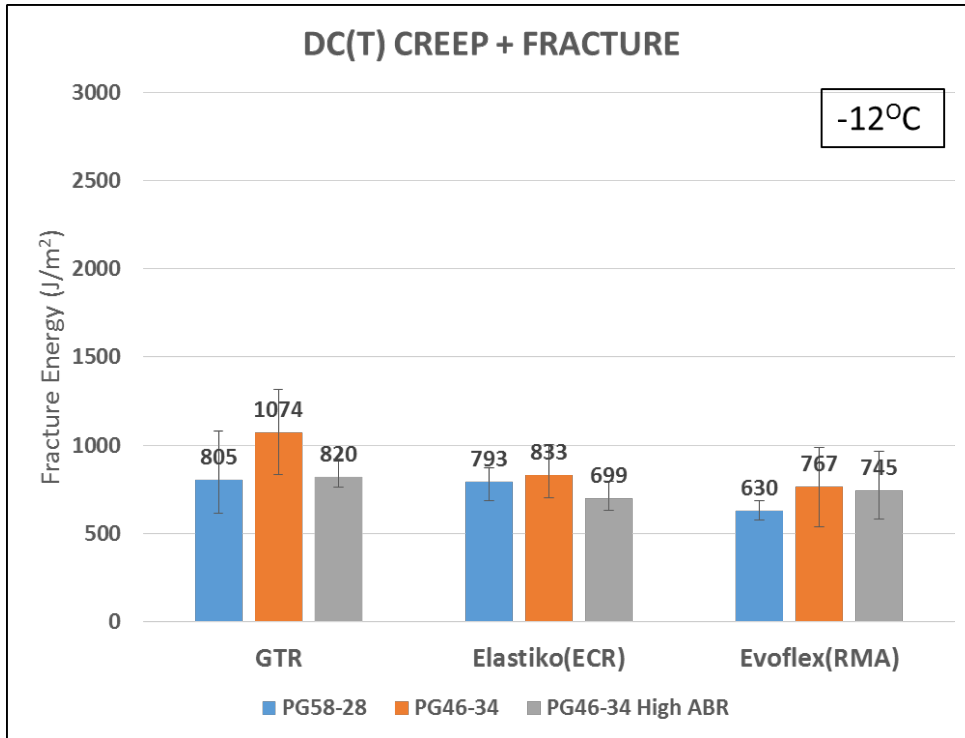
Figure 22. Creep compliance master curve for Evoflex (RMA) field cores

The m-values of the field core mixes are shown in Table 9, which offer insight to the relaxation properties of the mixes. The softer binder system show the highest m-value, as was expected. It is encouraging to infer from the m-values of the mixes that the addition of more recycled content does not affect the ability of the mix to relieve stresses drastically.

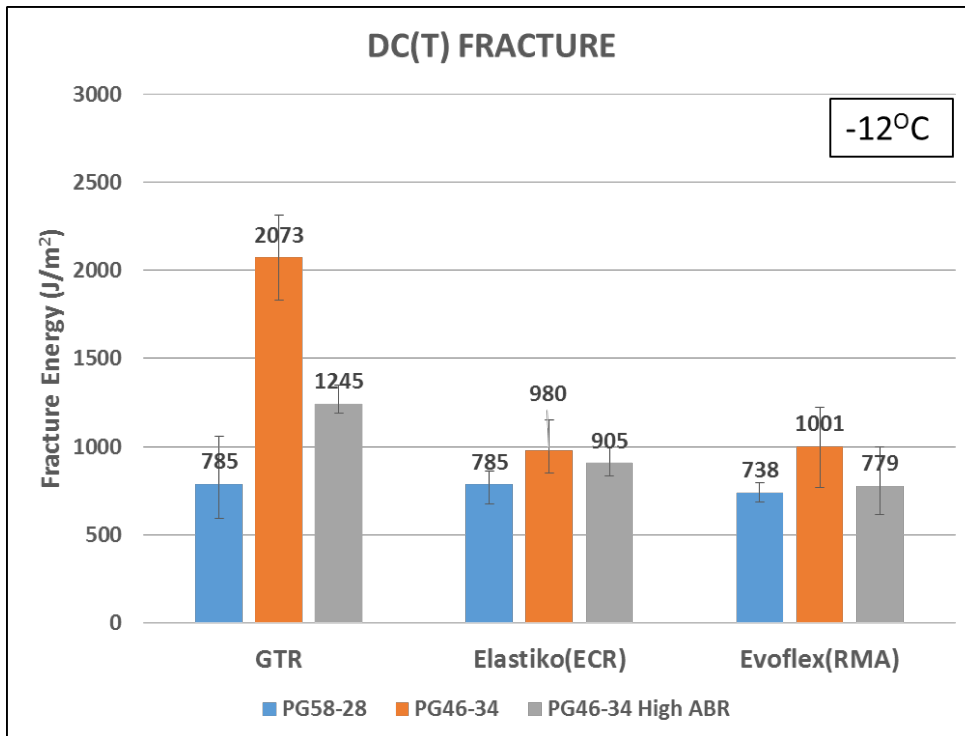
Table 9. m-value for field cores

	PG58-28	PG-46-34	PG46-34 High ABR
<b>GTR</b>	0.430	0.590	0.507
<b>Elastiko (ECR)</b>	0.460	0.517	0.447
<b>Evoflex (RMA)</b>	0.397	0.507	0.328

The results for DC(T) fracture energy test done after the DC(T) creep compliance testing for the field cores are shown in Fig. 23. In general, the fracture energy after creep compliance testing is lower than the fracture energy calculated without any creep compliance testing. Table 10 captures this through calculation of a damage parameter. The decrease in fracture energy could be attributed to two reasons: a. there could be some damage in the specimen during the creep loading, and b. since there is no relaxation time between the creep compliance at -12°C and the fracture energy test at the same temperature, the specimen might behave stiffer than usual during the fracture test resulting in lower fracture energy values.



a



b

Figure 23. a) DC(T) fracture energy values after creep testing for field cores b) DC(T) fracture energy test results for field cores without any creep compliance testing

Table 10. Damage percentages of field cores

	PG of Binder	DC(T) Creep+Fracture	DC(T) Fracture	Damage
		J/m <sup>2</sup> (A)	J/m <sup>2</sup> (B)	(%) ((B-A)/B)
	PG58-22	805	785	-3%
	PG46-34	1074	2073	48%
	PG46-34 High ABR	820	1245	34%
	PG58-22	793	785	-1%
	PG46-34	833	980	15%
	PG46-34 High ABR	699	905	23%
	PG58-22	630	738	15%
	PG46-34	767	1001	23%
	PG46-34 High ABR	745	779	4%

## Appendix B: Acoustic Emission Testing

Acoustic emission (AE) testing is a Non-Destructive Test (NDT) to characterize mixes on the basis of thermal cracking resistance [15]–[17]. When an asphalt mix specimen is subjected to low temperatures, the mix transitions from a brittle-ductile state to a quasi-brittle state. This lowers the fracture resistance of the mix and allows rapid formation of cracks within the mix structure. The formation of cracks and their subsequent crack growth through the structure releases strain energy in the form of transient stress waves, i.e. acoustic emissions (AE events), which can be detected within short ranges using AE piezoelectric sensors. The AE test method ‘listens’ to these emission events. Fig. 24 describes the AE concept [18]. The data is used to extract the embrittlement temperature information of the mix. A typical plot from the AE test has been shown in Fig. 25. The temperature corresponding to the first peak energy level event (above a prescribed threshold) is defined as the Embrittlement Temperature. One of the main advantages of AE testing is that it does not require any additional specimen fabrication; it can use the two broken halves of the DC(T) specimen.

The only caveat in using the tested DC(T) specimen is that the specimen could have been subjected to the embrittlement temperature while fracture testing. However, given that the DC(T) testing was performed at  $-12^{\circ}\text{C}$  and  $-18^{\circ}\text{C}$ , and the binders used in the mixes had Performance Grade Low Temperature (PGLT) much lower than  $-18^{\circ}\text{C}$ , it is safe to assume that DC(T) temperatures would not affect the embrittlement temperature values.

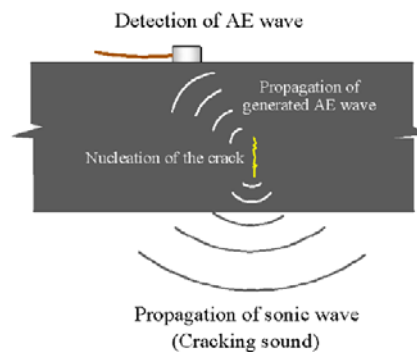


Figure 24. Working concept of Acoustic Emission Method[18]

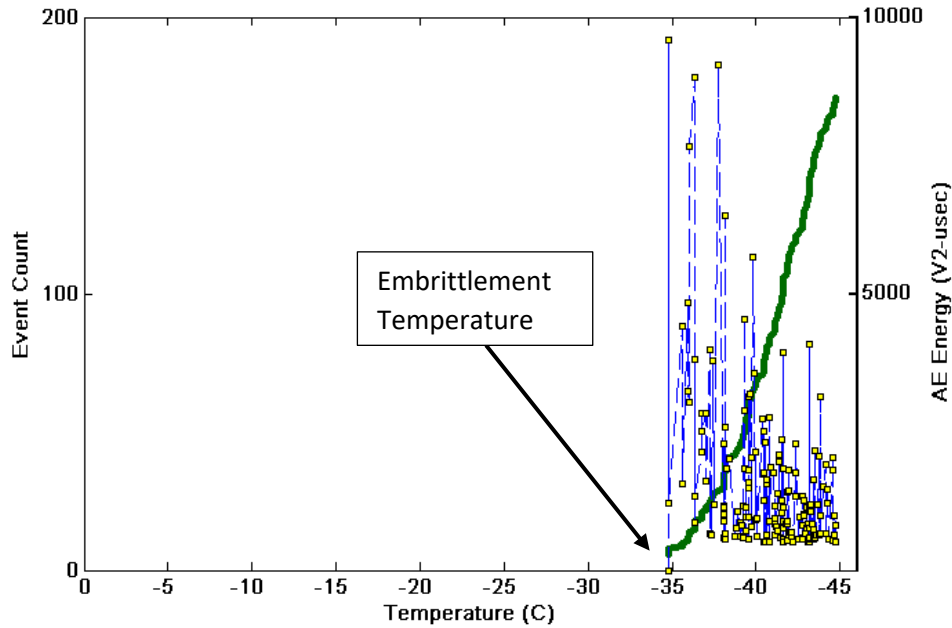


Figure 25. Typical AE plot [18]

### Acoustic Emission Testing Results

Fig. 26-27 show the plots of embrittlement temperatures for samples extracted from field cores and gyratory compacted mixtures, respectively. The field cores have shown cooler embrittlement temperatures than the corresponding gyratory samples. In the case of GTR field cores, the embrittlement temperatures are very close to their PGLT. The other two mixture types, however, show a warmer embrittlement temperature than the PGLT when a softer binder is used. There is no general trend to show the effect of high ABR on the embrittlement temperature of the mixes for the field cores. For the gyratory samples, the trend is similar to the DC(T) fracture energy. The use of softer binder leads to cooler embrittlement temperature, and the addition of recycled asphalt leads to a warmer embrittlement temperature. This gravitates more towards the expected results as the addition of softer binder increases the ductile part of the mix and should result in cooler embrittlement temperatures. The addition of recycled particles stiffens the mix, and hence warmer embrittlement temperatures should be seen. It is difficult to point out one single factor that could lead to the difference in trends observed in the samples extracted from field cores and gyratory compacted mixtures. One possible reason could be the difference of compaction energy. The replicates tested could have undergone some changes due to field factors, such as change in moisture content, or addition of sand/silt resulting in slight changes in mix gradation, change in binder content, or differences in short-term aging. The test results are summarized in Table 11.

It is important to mention that to obtain some embrittlement temperature values from the data, some adjustments were made – in some replicates the energy level observed was low and hence the threshold to define the embrittlement temperature regarding energy of an event was lowered; in some replicates, the initial events showed spikes in energy which were considered as noise and ignored. It was expected that the gyratory specimens would show cooler embrittlement temperatures than the field cores based on the fracture energy that was seen in Fig. 22-23. However, in case of the field cores, there were initial energy spikes quite early on the temperature scale, and those spikes were strong enough to cross the set threshold for embrittlement temperature. The gyratory samples showed similar behavior, but the energy spikes were sporadic and isolated - it was easy to identify them as noise/isolated events and filter them out. One possible reason for the early energy spikes (and low embrittlement temperature) could be the presence of rubber nodules in the mix that could give out AE waves at a much warmer temperature than the asphalt mastic.

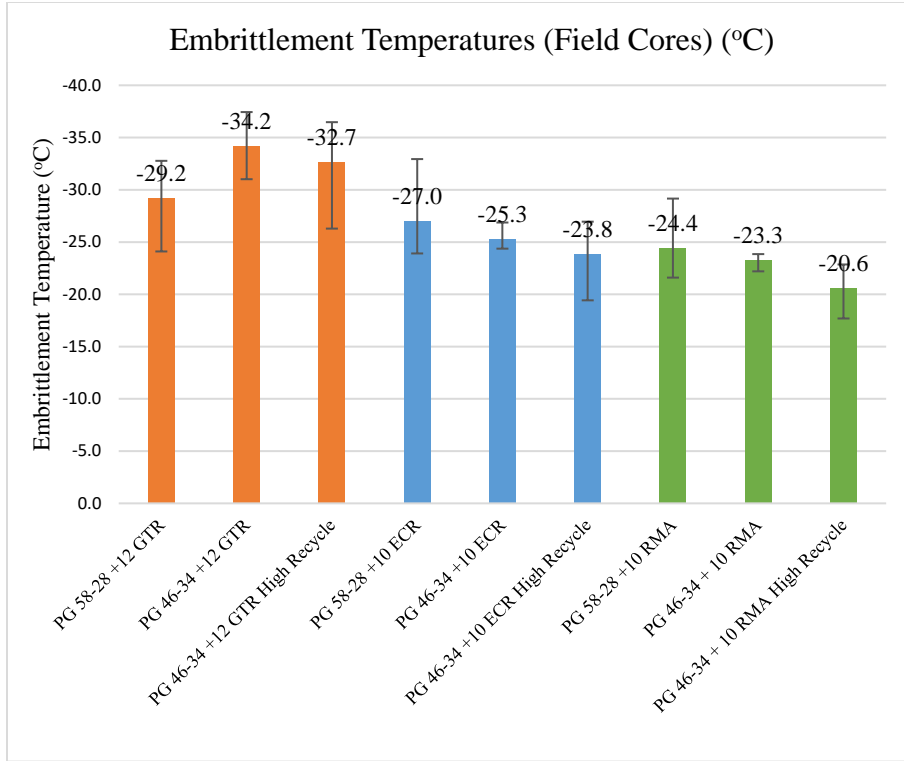


Figure 26. Embrittlement temperatures of field cores from AE testing

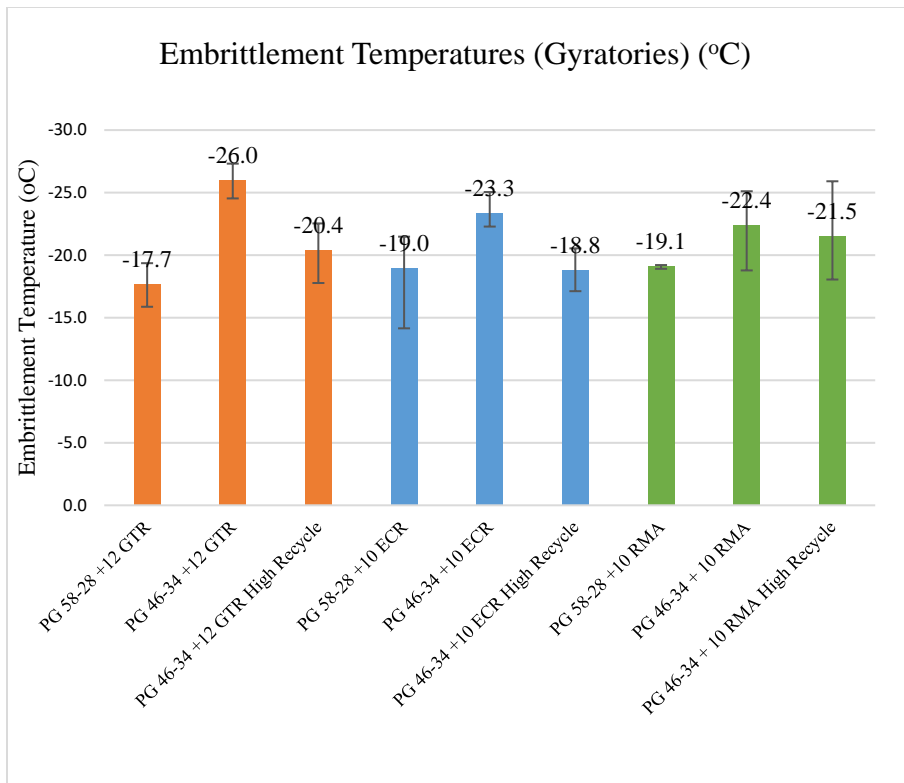


Figure 27. Embrittlement temperatures of gyratory samples from AE testing

Table 11. Acoustic Emission Testing - Embrittlement Temperatures for mixes

SMA Surface Friction Mixture	Embrittlement Temperature (°C)					
<b>Field Cores</b>						
<b>Seneca GTR</b>	<b>Rep 1</b>	<b>Rep 2</b>	<b>Rep 3</b>	<b>AVG</b>	<b>Std. Dev</b>	<b>COV</b>
PG 58-28 +12 GTR	-32.8	-24.1	-30.7	-29.2	4.5	15%
PG 46-34 +12 GTR	-37.4	-34.1	-31.0	-34.2	3.2	9%
PG 46-34 +12 GTR High Recycle	-36.5	-26.3	-35.3	-32.7	5.6	17%
<b>Elastiko 100</b>						
PG 58-28 +10 ECR	-32.9	-23.9	-24.2	-27.0	5.1	19%
PG 46-34 +10 ECR	-24.4	-26.9	-24.7	-25.3	1.4	5%
PG 46-34 +10 ECR High Recycle	-25.1	-19.4	-27.0	-23.8	3.9	16%
<b>Evoflex RMA</b>						
PG 58-28 +10 RMA	-22.4	-21.6	-29.2	-24.4	4.1	17%
PG 46-34 + 10 RMA	-23.7	-23.8	-22.2	-23.3	0.9	4%
PG 46-34 + 10 RMA High Recycle	-21.3	-17.7	-22.9	-20.6	2.7	13%
<b>Gyratory Samples</b>						
<b>Seneca GTR</b>	<b>Rep 1</b>	<b>Rep 2</b>	<b>Rep 3</b>	<b>AVG</b>	<b>Std. Dev</b>	<b>COV</b>
PG 58-28 +12 GTR	-19.4	-15.9	-17.9	-17.7	1.7	10%
PG 46-34 +12 GTR	-24.5	-26.2	-27.3	-26.0	1.4	5%
PG 46-34 +12 GTR High Recycle	-17.8	-20.8	-22.5	-20.4	2.4	12%
<b>Elastiko 100</b>						
PG 58-28 +10 ECR	-14.1	-21.5	-21.2	-19.0	4.2	22%
PG 46-34 +10 ECR	-25.0	-22.7	-22.3	-23.3	1.5	6%
PG 46-34 +10 ECR High Recycle	-18.7	-20.5	-17.1	-18.8	1.7	9%
<b>Evoflex RMA</b>						
PG 58-28 +10 RMA	-19.1	-18.9	-19.2	-19.1	0.2	1%
PG 46-34 + 10 RMA	-25.1	-23.2	-18.8	-22.4	3.2	15%
PG 46-34 + 10 RMA High Recycle	-25.9	-20.5	-18.1	-21.5	4.0	19%

## Appendix C: Post-Cracking Correction Factor

Due to the limitation with the new block circular saw used in fabricating the specimens, a slightly wider edge had to be made. To keep the specimens' ligament length similar to the standard, the notch length was decreased, while the drilled holes were fabricated according to the standard. With this fabrication, the loading pins were closer to the crack tip and consequently the Mode-I crack in the specimen appears at a lower CMOD value than the standard specimen giving a lower fracture energy value. Thus, a correction factor was needed for the non-standard specimens.

The correction factor devised would be a function of the Crack Mouth Opening Displacement and notch length. Further, the correction factor will decrease and eventually die out. In this study, a linear function was considered to be representative of the correction factor. The maximum correction factor ( $C_{fmax}$ ) was assumed to be the ratio of the notch lengths of the specimens. Among the boundary conditions, the correction factor would be maximum at the start of crack propagation (at  $\delta_c$ ) and it would be 1 at the end of the crack propagation (at  $\delta_f$ ) (Fig. 21). The function will be constant till the specimen reaches the peak load (at  $\delta_c$ ) and then it will linearly decrease to 1.



Figure 28. DC(T) specimens,  
a) standard specimen with notch length = b,  
b) non-standard specimen with notch length = b<sub>1</sub>

Maximum Correction Factor =  $C_{fmax} = b/b_1$ , where  $b > b_1$ ;  $b/b_1 > 1$

Boundary Conditions:

For CMOD(t) at  $\delta_c$ ,  $C_f(t) = C_{fmax}$  ..... (1)

For CMOD(t) at  $\delta_f$ ,  $C_f(t) = 1$  ..... (2)



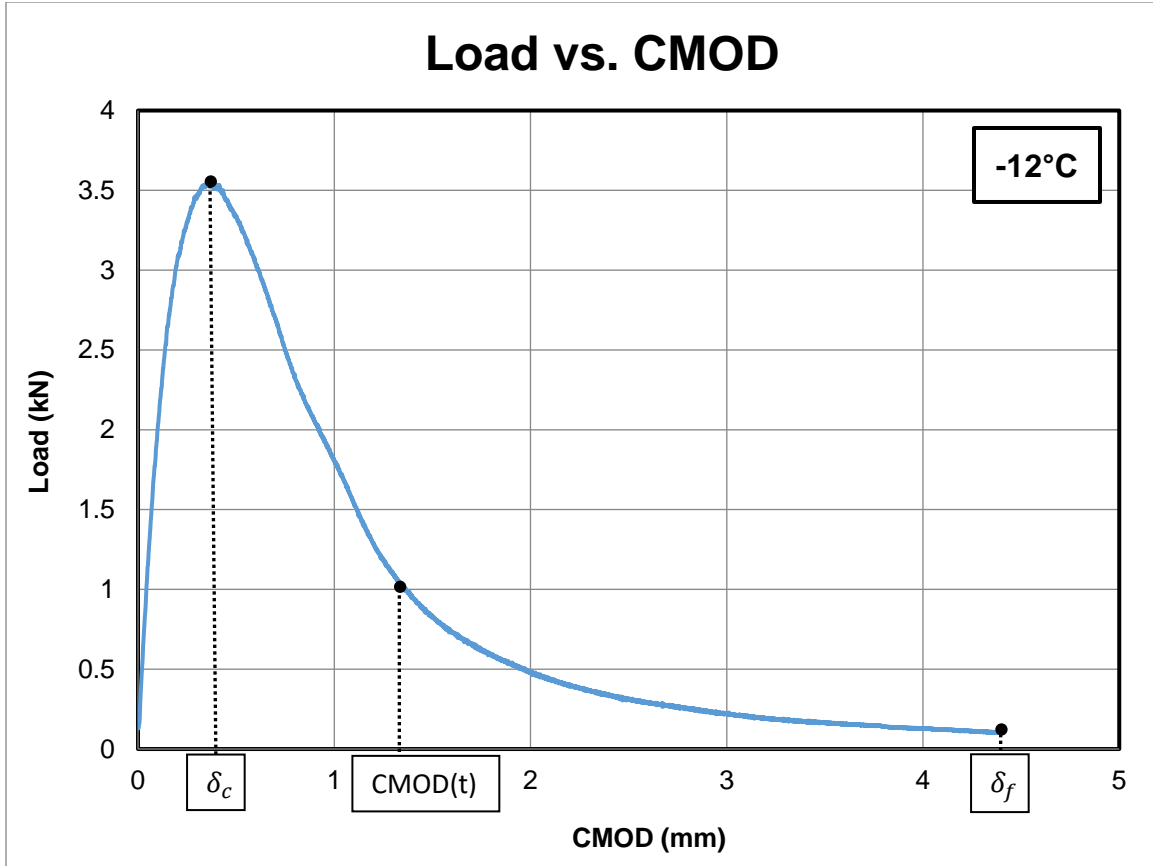


Figure 29. Typical Load-CMOD curve showing crack propagation stages

$C_f$  will depend on the relative position of CMOD in the Load-CMOD curve with respect to  $\delta_c$  and  $\delta_f$ . Using the boundary conditions and other constitutive inferences, the following function was devised that satisfied all the conditions-

$$C_i(t) = C_{fmax} \left( 1 - \frac{CMOD(t) - \delta_c}{\delta_f - \delta_c} \right)$$

$$\text{At } CMOD(t) = \delta_c, C_i(t) = C_{fmax} \left( 1 - \frac{\delta_c - \delta_c}{\delta_f - \delta_c} \right) = C_{fmax}$$

$$\text{At } CMOD(t) = \delta_f, C_i(t) = C_{fmax} \left( 1 - \frac{\delta_f - \delta_c}{\delta_f - \delta_c} \right) = C_{fmax}^0 = 1$$

Fig. 30 shows the typical correction factor function used to correct the fracture energy obtained from the non-standard specimen. Fig. 31 shows the change in the fracture energy before and after using the correction factor.

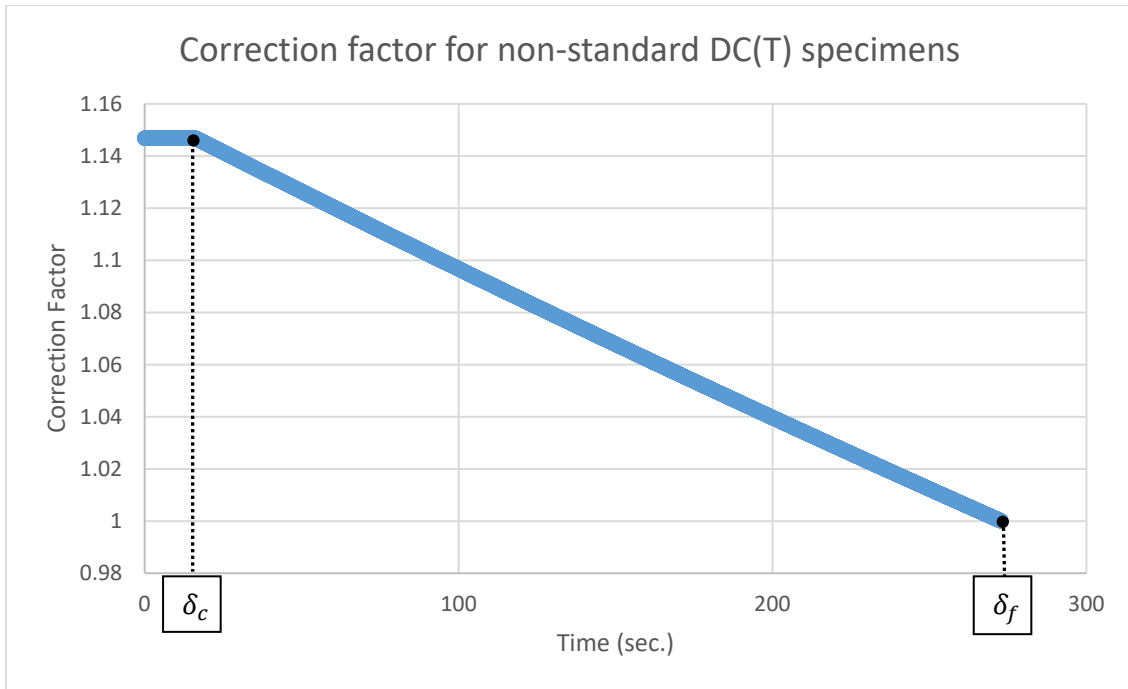


Figure 30. General correction factor function

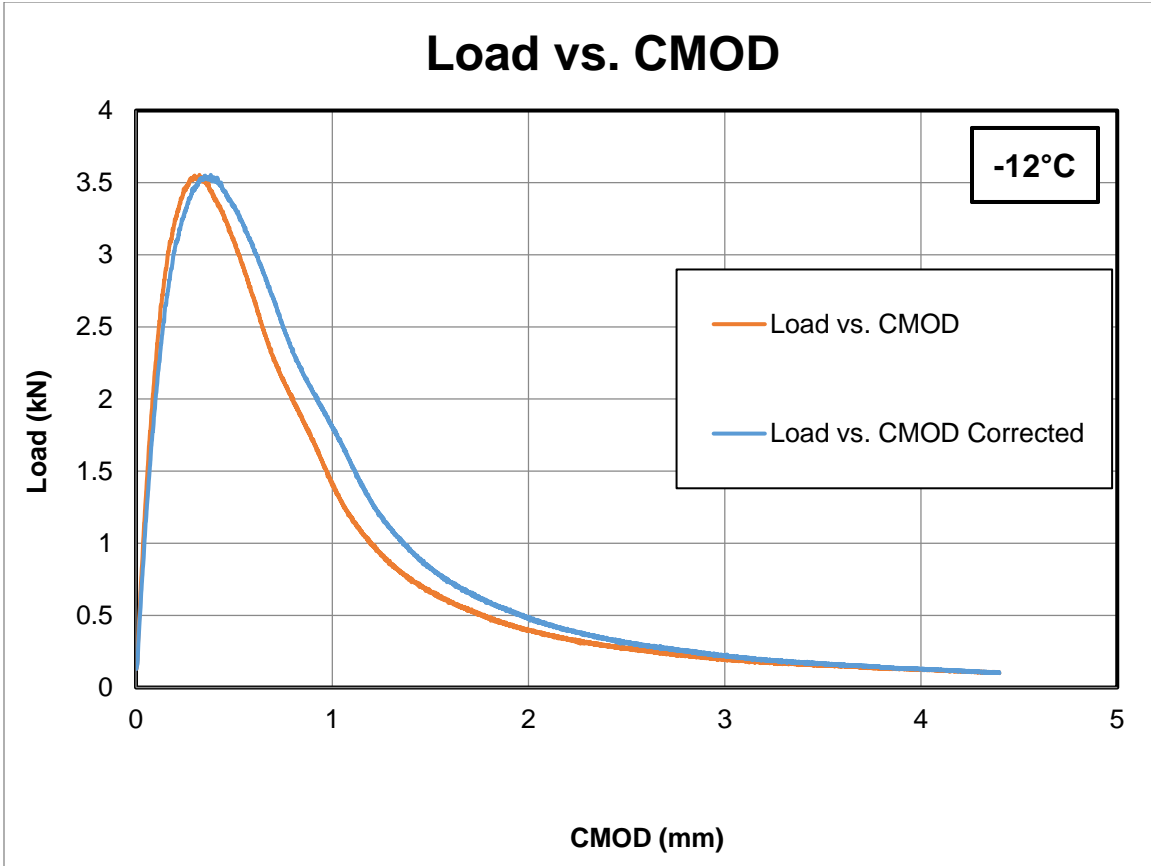


Figure 31. Load-CMOD plot with and without correction factor

## Appendix D: Remaining Sample Inventory

Item	Location	Quantity	Description/Notes
Bartlett CM-14	NEL shelves room	38	5 gal buckets
Bartlett CM-16	NEL shelves room	27	5 gal buckets
Bartlett RAP	NEL shelves room	20	5 gal buckets
Bartlett RAS	NEL shelves room	9	5 gal buckets
Bartlett loose mix	NEL shelves room	18	Burlap sacks
BP Bartlett 58-28 10% Evoflex	NEL shelves room	3	5 gal buckets
BP Bartlett 46-34 10% Evoflex	NEL shelves room	2	5 gal buckets
PG Bartlett 58-28 12% GTR	NEL shelves room	14	Small binder cans
PG Bartlett 46-34 12% GTR	NEL shelves room	16	Small binder cans
GTR	NEL shelves room	2	Small ziplocks
GTR	NEL shelves room	1	Large ziplock in box
Gyratories*	NEL shelves room	122	64 left at UIUC+25 left at Mizou
Cores	NEL shelves room	108	
*3 unlabelled			

# Appendix E: Mix Designs





DOT Lab Verification No.:  DATE: **March 25 2016**

Ver. 11.00.02.26.14

Plant Location

477-10 Curran DeKalb

18436R SMA SURFACE 12.5 REC

90WMA1633

Field Bin #	#7	#8	#5	#4	#3	#2	#1	MF	FRAP #4	RA# #3	RCY	RCY	ASPHALT
Size	030CUM18	030CUM14	030CUM14					04MFR02	017FRAB00	017FRAB00			46-54 OTR
Source (PROD #)	61938-01	62462-25	62462-25					477-10	477-10	477-10			1757-46
(NAME)	MAT-X	Milwaukee	Milwaukee					Curran	Southwind	Southwind			Seneca
(LOC)	Stirling	Waterloo	Waterloo					DeKalb	DeKalb	DeKalb			Lemont
(ADD. INFO)													46-54 OTR
Aggregate Blend:	18.0	0.0	56.3	0.0	0.0	0.0	0.0	3.5	16.0	5.6	0.0	0.0	PG 7B-22
Minire Blend:	16.9	0.0	53.5	0.0	0.0	0.0	0.0	3.3	16.2	7.0	0.0	0.0	PG 7B-22
													100.0
													100.0

Agg No.	#7	#8	#5	#4	#3	#2	#1	MF	FRAP #4	RA# #3	RCY	RCY	Aggregate Blend	Minire Comp
1" (25.0mm)	100.0	100.0	100.0	100.0	100.0	100.0	100.0	100.0	100.0	100.0	100.0	100.0	100.0	100
3/4" (18.0mm)	100.0	100.0	100.0	100.0	100.0	100.0	100.0	100.0	100.0	100.0	100.0	100.0	100.0	100
1/2" (12.5mm)	100.0	100.0	72.8	100.0	100.0	100.0	100.0	100.0	100.0	100.0	100.0	100.0	100.0	82-100
3/8" (9.5mm)	85.0	100.0	29.2	100.0	100.0	100.0	100.0	100.0	100.0	100.0	100.0	100.0	100.0	66 max
No.4 (4.75mm)	25.0	100.0	2.0	100.0	100.0	100.0	100.0	100.0	98.0	86.0	100.0	100.0	100.0	30-20
No.8 (2.36mm)	5.0	100.0	1.8	100.0	100.0	100.0	100.0	100.0	73.0	62.0	100.0	100.0	100.0	22
No.16 (1.18mm)	2.0	100.0	1.4	100.0	100.0	100.0	100.0	100.0	62.5	52.0	100.0	100.0	100.0	17
No.30 (600um)	2.0	100.0	1.4	100.0	100.0	100.0	100.0	100.0	37.5	24.0	100.0	100.0	100.0	14
No.60 (300um)	2.0	100.0	1.3	100.0	100.0	100.0	100.0	100.0	26.5	16.0	100.0	100.0	100.0	11
No.100 (150um)	2.0	100.0	1.3	100.0	100.0	100.0	100.0	100.0	17.0	9.0	100.0	100.0	100.0	9
No.200 (75um)	1.5	100.0	1.1	100.0	100.0	100.0	100.0	90.0	12.0	25.5	100.0	100.0	100.0	7.5
Bulk Sp Gr	3.375	1.000	2.682	1.000	1.000	1.000	1.000	2.990	2.680	2.402	1.000	1.000	2.758	Duct/AB
Absorption, %	1.75	1.00	0.40	1.00	1.00	1.00	1.00	1.00	1.00	1.00	1.00	1.00	0.69	Ratio
													1.042	SP GR AB
													1.24	

SUMMARY OF SUPERPAVE GYRATORY DESIGN DATA

DATA for N-46c	AB, % MIX	Gmb	Gmm	Voide (Pa)	VMA	VFA	Vbe	Pbe	Pba
MIX 1	6.5	2.186	2.580	16.3	25.1	38.1	8.83	4.88	0.88
MIX 2	6.0	2.188	2.593	14.2	25.1	43.2	10.84	5.14	0.91
MIX 3	6.5	2.209	2.540	13.0	25.1	48.1	12.08	5.70	0.88
MIX 4	7.0	2.221	2.535	12.0	25.1	52.1	13.07	6.13	0.84

DATA for N-46c	Gmb	Gmm	%VOIDS (Pa)	VMA	VFA	Vbe	Pbe	Pba	Occ
MIX 1	6.5	2.454	4.8	16.9	68.4	11.05	4.98	2.822	0.88
MIX 2	6.0	2.471	3.8	16.8	77.3	12.19	5.14	2.826	0.91
MIX 3	6.5	2.462	2.3	16.9	65.5	14.88	5.70	2.822	0.86
MIX 4	7.0	2.463	1.3	16.9	62.0	14.87	6.13	2.828	0.84

OPTIMUM DESIGN DATA @ Nodes	AB	Gmb	Gmm	%VOIDS (Pa)	VMA	VFA	G88	G8b	TSR	RCY AB	Virgin AB	ABR
60	6.0	2.472	2.682	Target	16.8	77.8	2.827	2.768	0.88	2.82	3.21	48.8
603				3.6								
REMARKS LINE 1	Hamburg & TSR Made With Warm Mix											
REMARKS LINE 2	Target J12 @ 2.4%											
REMARKS LINE 3	BITUMINOUS MIXTURE AGED 2 HOURS @ 355											

Lab Preparing Design:  Tested by:  Verified by:

Designing Lab:  CURDES19001

Designing Lab Name:  3.T.A.T.E. Reviewed by:  Final Approval:

90WMA1633



DOT Lab Verification No.:  DATE: **April 9 2016**

Ver: 11.00.02.20.14

Producer Number & Name → **477-10 Curran**

Plant Location

**DeKalb**

Material Code Number → **18436R SMA SURFACE 12.5 REC**

**90WMA1634**

Plant Blt #	#7	#8	#5	#4	#3	#2	#1	MF	FRAP #4	RA3 #5	RCY	RCY	ASPHALT
Source (PROD #)	030C418	032C414	032C414					00-MF02	017FR0400	017FR05			POSS-23-10 ECR
(NAME)	5198C-J1	5240C-25	5240C-25					477-10	477-10	081E-01			0827-10
(LOC)	Sterring	Michels	Michels					Curran	Southwind	Barfield			B.P.
(ADD. INFO)		Waterloo	Waterloo					DeKalb	DeKalb	Barfield			Barfield
										24.6	0.0	0.0	SB-28-10 ECR
													< AB in PLAP
Aggregate Blend:	25.0	0.0	50.5	0.0	0.0	0.0	0.0	4.5	12.0	4.0	0.0	0.0	PG 78-22
Mixture Blend:	27.2	0.0	47.5	0.0	0.0	0.0	0.0	4.2	12.1	5.0	0.0	0.0	Totals ↓
													100.0
													100.0

Agg No.	#7	#8	#5	#4	#3	#2	#1	MF	FRAP #4	RA3 #5	RCY	RCY	Mixture Comp
Sieve Size													Blend
1" (25.0mm)	100.0	100.0	100.0	100.0	100.0	100.0	100.0	100.0	100.0	100.0	100.0	100.0	100
3/4" (19.0mm)	100.0	100.0	100.0	100.0	100.0	100.0	100.0	100.0	100.0	100.0	100.0	100.0	100
1/2" (12.5mm)	100.0	100.0	100.0	100.0	100.0	100.0	100.0	100.0	100.0	100.0	100.0	100.0	88
3/8" (9.5mm)	83.0	100.0	72.8	100.0	100.0	100.0	100.0	100.0	100.0	100.0	100.0	100.0	85 max
No.4 (4.75mm)	25.0	100.0	2.0	100.0	100.0	100.0	100.0	100.0	89.0	86.0	100.0	100.0	29
No.8 (2.36mm)	3.9	100.0	1.8	100.0	100.0	100.0	100.0	100.0	73.0	82.0	100.0	100.0	19
No.16 (1.18mm)	2.9	100.0	1.5	100.0	100.0	100.0	100.0	100.0	62.5	75.0	100.0	100.0	15
No.30 (500µm)	2.9	100.0	1.4	100.0	100.0	100.0	100.0	100.0	37.5	54.0	100.0	100.0	12
No.60 (250µm)	2.9	100.0	1.4	100.0	100.0	100.0	100.0	100.0	35.5	46.0	100.0	100.0	11
No.100 (150µm)	2.0	100.0	1.3	100.0	100.0	100.0	100.0	95.0	17.0	32.0	100.0	100.0	9
No.200 (75µm)	1.8	100.0	1.1	100.0	100.0	100.0	100.0	90.0	12.0	26.5	100.0	100.0	7.5
Bulk Sp Gr	3.376	1.500	2.982	1.000	1.000	1.000	1.000	2.900	2.800	2.802	1.000	1.000	2.854
Absorption, %	1.70	1.00	0.40	1.00	1.00	1.00	1.00	1.00	1.00	1.00	1.00	1.00	0.81
													1.842
													1.28

SUMMARY OF SUPERPAVE GYRATORY DESIGN DATA

DATA FOR MIXTURE	AB, %MKX	Gmb	Gmm	Voids (P)	VMA	VFA	Vbe	Vbe	Pbe	Pbe
MIX.1	6.5	0.000	0.000	0.0	0.0	0.0	0.0	0.0	#DIV/0!	#DIV/0!
MIX.2	6.0	2.828	2.828	13.0	24.2	48.4	11.25	5.12	0.84	0.84
MIX.3	6.5	0.000	0.000	0.0	0.0	0.0	0.0	0.0	#DIV/0!	#DIV/0!
MIX.4	7.0	0.000	0.000	0.0	0.0	0.0	0.0	0.0	#DIV/0!	#DIV/0!

DATA FOR M-ONE	Gmb	Gmm	Voids (P)	VMA	VFA	Vbe	Vbe	Pbe	Pbe
MIX.1	6.5	0.000	0.000	0.0	0.0	0.0	0.0	0.0	#DIV/0!
MIX.2	6.0	2.827	2.828	3.4	15.9	78.8	12.47	5.12	2.908
MIX.3	6.5	0.000	0.000	0.0	0.0	0.0	0.0	0.0	#DIV/0!
MIX.4	7.0	0.000	0.000	0.0	0.0	0.0	0.0	0.0	#DIV/0!

OPTIMUM DESIGN DATA @ 80	Gmb	Gmm	%VOIDS (P)	VMA	VFA	Gsb	TSR	RCY AB	Virgin AB	ABR
#VALUE	6.0	2.827	2.828	3.4	15.9	78.8	12.47	5.12	2.907	33.9
REMARKS LINE 1	One Point Design									
REMARKS LINE 2	Integrity J13 @ 2.4%									
			Target							HOURS @
			3.4							358
										BITUMINOUS MIXTURE AGED
										2

Lab Preparing Design:   
 Designing Lab Name: CURDE18002  
 Designing Lab Name: S.T.A.T.E.  
 Tested by:   
 Reviewed by:   
 Verified by:   
 Final Approval:

90WMA1634

Ver. 11.00-02-20-14  
 DATE: April 3 2016

18436R SMA SURFACE 12.5 REC  
 Curran DeKalb  
 Plant Location

477-10  
 90WMA1635

Plant Bin #	#7	#8	#9	#5	#4	#3	#2	#1	MF	FRAP #4	RAS #3	RCY	RCY	ASPHALT
038CM18	0.0	50.5	0.0	0.0	0.0	0.0	0.0	0.0	4.5	04MRF02	017FM000	100.0	100.0	PAM-2.4-10 EGR
Source (PROD #)	6195E-01	6240C-25							477-10	477-10	0618-01	100.0	100.0	6827-03
(NAME)	MKT X	Mix							Curran	Curran	Boothwick	100.0	100.0	B.P.
(LOC)	Sharing	Widened							Durand	Durand	Boothwick	100.0	100.0	Barfield
(ADD. INFO)											24.6	0.0	0.0	AB 54-10 EGR
Aggregate Blend:	25.0	0.0	50.5	0.0	0.0	0.0	0.0	0.0	4.5	12.0	4.0	0.0	0.0	PS 14-25
Mixture Blend:	27.2	0.0	47.5	0.0	0.0	0.0	0.0	0.0	4.2	12.1	5.0	0.0	0.0	PS 14-25
														100.0
														100.0

Agg No.	#7	#8	#9	#5	#4	#3	#2	#1	MF	FRAP #4	RAS #3	RCY	RCY	Aggregate Blend	Mixture Comp
1" (25.0mm)	100.0	100.0	100.0	100.0	100.0	100.0	100.0	100.0	100.0	100.0	100.0	100.0	100.0	100	100
3/4" (19.0mm)	100.0	100.0	100.0	100.0	100.0	100.0	100.0	100.0	100.0	100.0	100.0	100.0	100.0	100	100
1/2" (12.5mm)	100.0	100.0	100.0	100.0	100.0	100.0	100.0	100.0	100.0	100.0	100.0	100.0	100.0	98	82-100
3/8" (9.5mm)	93.0	100.0	100.0	29.2	100.0	100.0	100.0	100.0	100.0	98.0	98.0	100.0	100.0	62	66 max
No.4 (4.75mm)	25.0	100.0	100.0	2.0	100.0	100.0	100.0	100.0	100.0	88.0	88.0	100.0	100.0	29	20-30
No.8 (2.36mm)	3.0	100.0	100.0	1.8	100.0	100.0	100.0	100.0	100.0	73.0	82.0	100.0	100.0	19	18-24
No.18 (1.18mm)	2.0	100.0	100.0	1.5	100.0	100.0	100.0	100.0	100.0	62.6	76.0	100.0	100.0	16	12-16
No.30 (800µm)	2.0	100.0	100.0	1.4	100.0	100.0	100.0	100.0	100.0	37.5	54.0	100.0	100.0	12	12-16
No.60 (300µm)	2.0	100.0	100.0	1.4	100.0	100.0	100.0	100.0	100.0	25.5	46.0	100.0	100.0	11	12-16
No.100 (150µm)	2.0	100.0	100.0	1.3	100.0	100.0	100.0	100.0	86.0	17.0	37.0	100.0	100.0	9	10-15
No.200 (75µm)	1.5	100.0	100.0	1.1	100.0	100.0	100.0	100.0	86.0	12.0	28.5	100.0	100.0	7.5	8-10
Bulk Sp Or	3.975	1.000	2.892	1.000	1.000	1.000	1.000	1.000	2.900	2.890	2.402	1.000	1.000	2.894	Dust/AB
Absorption, %	1.70	1.00	0.40	1.00	1.00	1.00	1.00	1.00	1.00	1.00	1.00	1.00	1.00	0.81	Ratio
														1.042	SP 0.9 AB

SUMMARY OF SUPERPAVE GYRATORY DESIGN DATA

DATA for N. Job	AB	MAK	Gmb	Gmm	Voids (%)	VMA	VFA	Vbe	Vbe	Vbe	Vbe	TSR	TSR	RCY AB	Virgin AB	ABR
MIX.1	6.6	0.000	2.374	2.623	13.5	24.6	46.5	11.25	6.18	0.89	0.89	0.00	0.00	2.97	4.83	33.8
MIX.2	6.0	0.000	2.628	2.623	0.0	0.0	0.0	0.0	0.0	0.0	0.0	0.00	0.00	0.00	0.00	0.00
MIX.3	6.6	0.000	2.374	2.623	13.5	24.6	46.5	11.25	6.18	0.89	0.89	0.00	0.00	2.97	4.83	33.8
MIX.4	7.9	0.000	0.000	0.000	0.0	0.0	0.0	0.0	0.0	0.0	0.0	0.00	0.00	0.00	0.00	0.00

DATA for N. Job	AB	MAK	Gmb	Gmm	Voids (%)	VMA	VFA	Vbe	Vbe	Vbe	Vbe	TSR	TSR	RCY AB	Virgin AB	ABR
MIX.1	6.6	0.000	2.374	2.623	13.5	24.6	46.5	11.25	6.18	0.89	0.89	0.00	0.00	2.97	4.83	33.8
MIX.2	6.0	0.000	2.628	2.623	0.0	0.0	0.0	0.0	0.0	0.0	0.0	0.00	0.00	0.00	0.00	0.00
MIX.3	6.6	0.000	2.374	2.623	13.5	24.6	46.5	11.25	6.18	0.89	0.89	0.00	0.00	2.97	4.83	33.8
MIX.4	7.9	0.000	0.000	0.000	0.0	0.0	0.0	0.0	0.0	0.0	0.0	0.00	0.00	0.00	0.00	0.00

OPTIMUM DESIGN DATA @ Nicks  
 GYRATIONS  
 VALUE: 6.0  
 TARGET: 3.7

REMARKS LINE 1 One Point Design  
 REMARKS LINE 2 Identify J12 @ 0.4%

Lab Preparing Design: IL  
 Designing Lab: CURDES 18002  
 Designing Lab Name: S.T.A.T.E.  
 Tested by: \_\_\_\_\_  
 Reviewed by: \_\_\_\_\_  
 Verified by: \_\_\_\_\_  
 Final Approval: \_\_\_\_\_

Ver. 11.00-02.20.14  
 IDOT Lab Verification No.:   
 DATE:   
 Plant Location

Producer Number & Name:    
 Material Code Number:

Prod Blk #	#7	#8	#5	#4	#3	#2	#1	MF	FRAP #4	RA# #3	RCY	RCY	ASPHALT
Source (PROD #)	030CM18	030CM14	030CM4					04MMS2	017FMAS0	017FMAS			46-34 ECR
(NAME)	5183E-21	5183E-22	5183E-23					477-10	017FMAS	017FMAS			8227-13
(LOC)	Spring	Winters	Winters					Curran	Scoutwood	Scoutwood			BP
(ADD. INFO)								DeKalb	DeKalb	DeKalb			Barrett
Aggregate Blend:	18.0	0.0	56.9	0.0	0.0	0.0	0.0	3.5	8.9	24.6	0.0	0.0	46-34 ECR
Mixture Blend:	16.9	0.0	53.5	0.0	0.0	0.0	0.0	3.3	16.0	5.6	0.0	0.0	Plan PG Grade -> PG 76-22
									16.2	7.0	0.0	0.0	PG 76-22
													Trial# 1
													Trial# 2
													Trial# 3

Agg No.	#7	#8	#5	#4	#3	#2	#1	MF	FRAP #4	RA# #3	RCY	RCY	Aggregate Blend	Mixture Comp
1" (25.0mm)	100.0	100.0	100.0	100.0	100.0	100.0	100.0	100.0	100.0	100.0	100.0	100.0	100.0	100
3/4" (18.0mm)	100.0	100.0	100.0	100.0	100.0	100.0	100.0	100.0	100.0	100.0	100.0	100.0	100.0	100
1/2" (12.5mm)	100.0	100.0	100.0	100.0	100.0	100.0	100.0	100.0	100.0	100.0	100.0	100.0	100.0	85-100
3/8" (9.5mm)	89.0	100.0	72.8	100.0	100.0	100.0	100.0	100.0	100.0	100.0	100.0	100.0	100.0	86
No.4 (4.75mm)	25.0	100.0	29.2	100.0	100.0	100.0	100.0	100.0	88.0	88.0	100.0	100.0	100.0	68
No.8 (2.36mm)	3.0	100.0	1.8	100.0	100.0	100.0	100.0	100.0	73.0	82.0	100.0	100.0	100.0	30
No.16 (1.18mm)	2.0	100.0	1.6	100.0	100.0	100.0	100.0	100.0	62.5	75.0	100.0	100.0	100.0	22
No.30 (800um)	2.0	100.0	1.4	100.0	100.0	100.0	100.0	100.0	37.5	64.0	100.0	100.0	100.0	14
No.60 (300um)	2.0	100.0	1.4	100.0	100.0	100.0	100.0	100.0	37.5	46.0	100.0	100.0	100.0	11
No.100 (150um)	2.0	100.0	1.3	100.0	100.0	100.0	100.0	85.0	17.0	37.0	100.0	100.0	100.0	9
No.200 (75um)	1.5	100.0	1.1	100.0	100.0	100.0	100.0	80.0	12.0	26.5	100.0	100.0	100.0	7.5
Bulk Sp Gr	3.376	1.000	2.862	1.000	1.000	1.000	1.000	2.900	2.860	2.402	1.000	1.000	2.758	Dual/AB
Absorption, %	1.78	1.90	0.40	1.00	1.00	1.00	1.00	1.00	1.90	1.95	1.00	1.00	0.88	Ratio
													SP OR AB	1.842
														1.24

SUMMARY OF SUPERPAVE GYRATORY DESIGN DATA

AB, % MIX	Gmb	Gmm	Voids (P <sub>v</sub> )	VMA	VFA	Vbe	Pbe	Pba	TSR Information		
									Conditioned	Unconditioned	
MIX 1	2.183	2.888	16.4	24.9	37.8	8.43	4.48	1.08	0.84	111.8	
MIX 2	2.208	2.887	14.1	24.8	43.3	6.07	0.89	1.06	0.84	111.8	
MIX 3	2.224	2.851	12.8	24.8	47.8	11.78	6.52	1.06	0.84	111.8	
MIX 4	2.242	2.830	11.4	24.4	53.4	13.00	6.04	1.03	0.84	111.8	
DATA for N-6%:											
MIX 1	2.468	2.893	6.3	16.9	88.7	10.68	4.48	2.898	1.08	111.8	
MIX 2	2.476	2.887	3.8	16.7	77.1	12.04	6.07	2.892	0.89	111.8	
MIX 3	2.490	2.851	2.4	16.6	84.7	13.19	6.52	2.897	1.06	111.8	
MIX 4	2.501	2.830	1.2	16.7	82.7	14.60	6.04	2.895	1.03	111.8	
OPTIMUM DESIGN DATA @ Voids											
AB	Gmb	Gmm	%VOIDS (P <sub>v</sub> )	VMA	VFA	G88	G88	TSR	RCY/AB	Virgin AB	ABR
60	2.476	2.888	Target: 3.8	16.6	77.8	2.892	2.760	0.84	2.82	3.21	48.8
REMARKS LINE 1: Hamburg & TSR Made With Warm Mix											
REMARKS LINE 2: Integrity J12 @ 3.4%											
HOURS @ 355											

Hamburg Wheel Information  
 Sample No. Phases: 20500  
 Sample Wheel Depth: 2.88

TSR Information  
 Conditioned: 105.7  
 Unconditioned: 111.8  
 TSR: 0.84  
 CA IHP Rating: 2  
 FA IHP Rating: 2  
 Additive Prod #:   
 Additive Product Name:   
 Additive %:

Tested by: \_\_\_\_\_  
 Designing Lab Name: COURDE 18002  
 Designing Lab Name: S.T.A.T.E.  
 Verified by: \_\_\_\_\_  
 Final Approval: \_\_\_\_\_

Ver. 11.04-02.20.14

DATE: April 9 2016

IDOT Lab Verification No.:

90WMA1637

Plant Location

DeKalb

477-10 Curran

18436R SMA SURFACE 12.5 REC

Material Code Number

477-10 Curran

DeKalb

18436R SMA SURFACE 12.5 REC

Plant Bin #	#7	#8	#5	#4	#3	#2	#1	MF	FRAP #4	RAA #5	RCY	RCY	RCY	APPROX
Size	0.075mm	0.075mm	0.075mm	0.075mm	0.075mm	0.075mm	0.075mm	0.075mm	0.075mm	0.075mm	100.0	100.0	100.0	100.0
Source (PROD #)	51358-21	52402-26	52402-26	52402-26	52402-26	52402-26	52402-26	52402-26	52402-26	52402-26	477-10	477-10	477-10	527-13
(NAME)	MAT-X	Mishels	Mishels	Mishels	Mishels	Mishels	Mishels	Mishels	Mishels	Mishels	Curran	Curran	Curran	B.P.
(LOC)	Shelby	Waterloo	Waterloo	Waterloo	Waterloo	Waterloo	Waterloo	Waterloo	Waterloo	Waterloo	DeKalb	DeKalb	DeKalb	Bartlett
(ADD. INFO)														66-28-10 RMA
Aggregate Blend:	25.0	0.0	50.5	0.0	0.0	0.0	0.0	4.5	8.9	24.6	0.0	0.0	0.0	< AB In RAP
Mixture Blend:	27.2	0.0	47.5	0.0	0.0	0.0	4.2	12.1	12.1	5.0	0.0	0.0	0.0	PG 75-22
														Total: 100.0

Agg No.	#7	#8	#5	#4	#3	#2	#1	MF	FRAP #4	RAA #5	RCY	RCY	RCY	Mixture Comp
sieve size	100.0	100.0	100.0	100.0	100.0	100.0	100.0	100.0	100.0	100.0	100.0	100.0	100.0	Space
1" (25.0mm)	100.0	100.0	100.0	100.0	100.0	100.0	100.0	100.0	100.0	100.0	100.0	100.0	100.0	100
3/4" (19.0mm)	100.0	100.0	100.0	100.0	100.0	100.0	100.0	100.0	100.0	100.0	100.0	100.0	100.0	82-100
1/2" (12.5mm)	100.0	100.0	100.0	100.0	100.0	100.0	100.0	100.0	100.0	100.0	100.0	100.0	100.0	86 max
3/8" (9.5mm)	85.0	100.0	29.2	100.0	100.0	100.0	100.0	100.0	99.0	88.0	100.0	100.0	100.0	20-30
No.4 (4.75mm)	25.0	100.0	2.0	100.0	100.0	100.0	100.0	100.0	73.0	82.0	100.0	100.0	100.0	18-24
No.8 (1.9mm)	3.0	100.0	1.5	100.0	100.0	100.0	100.0	100.0	52.5	75.0	100.0	100.0	100.0	15
No.16 (0.85mm)	2.0	100.0	1.4	100.0	100.0	100.0	100.0	100.0	37.6	54.0	100.0	100.0	100.0	12
No.30 (0.60mm)	2.0	100.0	1.4	100.0	100.0	100.0	100.0	100.0	26.6	46.0	100.0	100.0	100.0	11
No.60 (0.30mm)	2.0	100.0	1.3	100.0	100.0	100.0	100.0	100.0	17.0	37.0	100.0	100.0	100.0	9
No.100 (0.15mm)	1.8	100.0	1.1	100.0	100.0	100.0	100.0	86.0	12.0	24.5	100.0	100.0	100.0	7.5
No.200 (0.075mm)	1.8	100.0	1.1	100.0	100.0	100.0	100.0	86.0	12.0	24.5	100.0	100.0	100.0	7.5
Bulk Sp Gr	3.375	1.000	2.682	1.000	1.000	1.000	1.000	2.900	2.680	2.402	1.000	1.000	1.000	Duct/AB
Absorption, %	1.75	1.00	0.40	1.00	1.00	1.00	1.00	1.00	1.00	1.00	1.00	1.00	1.00	0.81
														Ratio
														1.042
														1.28

SUMMARY OF SUPERPAVE GYRATORY DESIGN DATA

DATA for N-Jct.	B	AB, MAX	Gmm	Voids (Pa)	VMA	VFA	Vbe	Vbe	Pbe	Pbe	Pbe
MIX 1	5.6	0.000	0.000	0.0	0.0	0.0	0.00	0.00	#DIV/0!	#DIV/0!	#DIV/0!
MIX 2	6.0	2.278	2.825	13.3	24.5	46.7	11.23	5.14	5.14	0.82	0.82
MIX 3	6.5	0.000	0.000	0.0	0.0	0.0	0.00	0.00	#DIV/0!	#DIV/0!	#DIV/0!
MIX 4	7.0	0.000	0.000	0.0	0.0	0.0	0.00	0.00	#DIV/0!	#DIV/0!	#DIV/0!

DATA for N-Jct.	B	Gmb	Gmm	%VOIDS (Pa)	VMA	VFA	G#	G#	G#	TSR	RCY AB	Virgin AB	ABR
MIX 1	5.6	0.000	0.000	0.0	0.0	0.0	0.00	0.00	0.00	0.00	#DIV/0!	#DIV/0!	#DIV/0!
MIX 2	6.0	2.632	2.625	3.5	18.0	77.9	12.48	5.14	3.907	0.82	0.82	0.82	30.9
MIX 3	6.5	0.000	0.000	0.0	0.0	0.0	0.00	0.00	#DIV/0!	#DIV/0!	#DIV/0!	#DIV/0!	#DIV/0!
MIX 4	7.0	0.000	0.000	0.0	0.0	0.0	0.00	0.00	#DIV/0!	#DIV/0!	#DIV/0!	#DIV/0!	#DIV/0!

BITUMINOUS DESIGN DATA @ Notes

GYRATIONS	AB	Gmb	Gmm	%VOIDS (Pa)	VMA	VFA	G#	G#	TSR	RCY AB	Virgin AB	ABR
80	6.0	2.631	2.625	3.5	18.0	77.9	12.48	5.14	3.907	0.82	0.82	30.9
6.0	6.0	2.631	2.625	3.5	18.0	77.9	12.48	5.14	3.907	0.82	0.82	30.9
One Point				3.5								
Target				3.5								
REMARKS LINE 1	One Point											
REMARKS LINE 2	Density J12 @ 0.4%											
REMARKS LINE 3	BITUMINOUS MIXTURE AGED 2 HOURS @ 355											

Lab Preparing Design: L  
 Designing Lab: MISH CURDES 18002  
 Designing Lab Name: S.T.A.T.E.  
 Tested by: \_\_\_\_\_  
 Reviewed by: \_\_\_\_\_  
 Verified by: \_\_\_\_\_  
 Final Approval: \_\_\_\_\_

90WMA1637

DATE: April 9 2016  
 90WMA1638

Product Number & Name → 477-10 Curran Dekalb  
 Material Code Number → 18436R SMA SURFACE 12.5 REC

Prod Bch #	#7	#8	#5	#4	#3	#2	#1	MF	FRAP #4	RA3 #3	RCY	RCY	ASPHALT
038CM18	632CM14	632CM14	632CM14	632CM14	632CM14	632CM14	632CM14	04AMP02	017FM040	017FM03	017FM03	017FM03	PO48-54+10 RMA
Source (PROD #)	6186K-01	632CM14	632CM14	632CM14	632CM14	632CM14	632CM14	477-10	477-10	9818-01	9818-01	9818-01	8827-13
(NAME)	Maxx	Maxx	Maxx	Maxx	Maxx	Maxx	Maxx	Curran	Curran	Southland	Southland	Southland	B.P.
(LOC)	Shoring	Shoring	Shoring	Shoring	Shoring	Shoring	Shoring	Dekalb	Dekalb	Dekalb	Dekalb	Dekalb	Shoring
(ADD. INFO)													48-54+10 RMA
Aggregate Blend:													4.03% RAP
25.0	0.0	50.5	0.0	0.0	0.0	0.0	0.0	4.5	12.0	4.0	0.0	0.0	Plain PO Gravel - PS 17-23
Mixture Blend:	27.2	0.0	47.5	0.0	0.0	0.0	0.0	4.2	12.1	5.0	0.0	0.0	Total: 100.0

App No.	#7	#8	#5	#4	#3	#2	#1	MF	FRAP #4	RA3 #3	RCY	RCY	Aggregate Blend	Mixture Comp Spec
1"	100.0	100.0	100.0	100.0	100.0	100.0	100.0	100.0	100.0	100.0	100.0	100.0	100	100
3/4"	100.0	100.0	100.0	100.0	100.0	100.0	100.0	100.0	100.0	100.0	100.0	100.0	100	100
1/2"	100.0	100.0	100.0	100.0	100.0	100.0	100.0	100.0	100.0	100.0	100.0	100.0	88	82-100
3/8"	100.0	100.0	100.0	100.0	100.0	100.0	100.0	100.0	100.0	100.0	100.0	100.0	86	86 max
No.4 (4.75mm)	2.0	100.0	2.0	100.0	100.0	100.0	100.0	100.0	88.0	86.0	100.0	100.0	29	20-30
No.8 (2.36mm)	3.0	100.0	1.8	100.0	100.0	100.0	100.0	100.0	73.0	82.0	100.0	100.0	19	16-24
No.16 (1.18mm)	2.0	100.0	1.6	100.0	100.0	100.0	100.0	100.0	62.5	75.0	100.0	100.0	15	12-18
No.30 (600µm)	2.0	100.0	1.4	100.0	100.0	100.0	100.0	100.0	37.5	54.0	100.0	100.0	12	12-18
No.60 (300µm)	2.0	100.0	1.4	100.0	100.0	100.0	100.0	100.0	25.5	45.0	100.0	100.0	11	10-15
No.100 (150µm)	2.0	100.0	1.3	100.0	100.0	100.0	100.0	95.0	17.0	37.0	100.0	100.0	9	8-10
No.200 (75µm)	1.5	100.0	1.1	100.0	100.0	100.0	100.0	90.0	12.0	26.5	100.0	100.0	7.5	8-10
Bulk Sto or Absorption, %	9.375	1.900	2.882	1.000	1.000	1.000	1.000	2.990	2.990	2.902	1.000	1.000	2.834	Duct/AB Ratio
	1.70	1.00	0.40	1.00	1.00	1.00	1.00	1.00	1.00	1.00	1.00	1.00	0.81	1.38
													SP GR AB	1.842

SUMMARY OF SUPERPAVE GYRATORY DESIGN DATA

AB, %MKX	Gmb	Gmm	Voids (Pv)	VMA	VFA	Vbe	Pbe	Pba
MIX.1	6.6	0.000	0.0	0.0	0.0	0.00	0.000	0.000
MIX.2	8.0	2.884	13.7	24.9	44.9	11.17	5.14	0.81
MIX.3	6.6	0.000	0.0	0.0	0.0	0.00	0.000	0.000
MIX.4	7.0	0.000	0.0	0.0	0.0	0.00	0.000	0.000

AB	Gmb	Gmm	Voids (Pv)	VMA	VFA	Vbe	Pbe	Pba
MIX.1	6.6	0.000	0.0	0.0	0.0	0.00	0.000	0.000
MIX.2	8.0	2.820	4.0	16.4	76.8	12.48	2.898	0.81
MIX.3	6.6	0.000	0.0	0.0	0.0	0.00	0.000	0.000
MIX.4	7.0	0.000	0.0	0.0	0.0	0.00	0.000	0.000

AB	Gmb	Gmm	%VOIDS (Pv)	VMA	VFA	Gsb	TSR	RCY AB	Virgin AB	ABR
80	8.0	2.820	4.0	16.4	76.8	2.87	4.03	33.8	33.8	33.8

REMARKS LINE 1: One Point  
 REMARKS LINE 2: 100% 212 @ 0.4%

Tested by: \_\_\_\_\_  
 Designing Lab Name: COURSE 6802  
 Designing Lab Name: STATE

Verified by: \_\_\_\_\_  
 Final Approval: \_\_\_\_\_

90WMA1638

Ver. 11.00-02.20.14  
 DATE: April 9 2016  
 90WMA1639

DOT Lab Verification No.:  
 477-10 Curran DeKalb  
 18436R SMA SURFACE 12.5 REC

Producer Number & Name  
 477-10 Curran DeKalb  
 Material Code Number  
 18436R SMA SURFACE 12.5 REC

Plant Location  
 ← Plant Location

Plant Bin #	#7	#8	#5	#4	#3	#2	#1	MF	FRAP #4	RA3 #3	RCY	RCY	ASPHALT
038CM19	038CM19	038CM14	038CM14	038CM14	038CM14	038CM14	038CM14	038CM14	038CM14	038CM14	038CM14	038CM14	46-54 RMA
Source (PROD #)	61852-51	52402-52	52402-52	52402-52	52402-52	52402-52	52402-52	52402-52	52402-52	52402-52	52402-52	52402-52	6027-15
(NAME)	MAT-X	Mohans	Mohans	Mohans	Mohans	Mohans	Mohans	Mohans	Mohans	Mohans	Mohans	Mohans	B.P.
(LOC)	Staring	Wenroco	Wenroco	Wenroco	Wenroco	Wenroco	Wenroco	Wenroco	Wenroco	Wenroco	Wenroco	Wenroco	Barbet
(ADD. INFO)													46-54 RMA
													< AB in RAP
													PG 74-22
Aggregate Blend:	18.0	0.0	56.3	0.0	0.0	0.0	0.0	3.5	15.0	5.6	0.0	0.0	100.0
Mixture Blend:	18.0	0.0	53.5	0.0	0.0	0.0	0.0	3.3	15.2	7.0	0.0	0.0	100.0
Totals:													

Agg No.	#7	#8	#5	#4	#3	#2	#1	MF	FRAP #4	RA3 #3	RCY	RCY	Mixture Comp
Sieve Size	100.0	100.0	100.0	100.0	100.0	100.0	100.0	100.0	100.0	100.0	100.0	100.0	Blend
1" (25.0mm)	100.0	100.0	100.0	100.0	100.0	100.0	100.0	100.0	100.0	100.0	100.0	100.0	100
3/4" (19.0mm)	100.0	100.0	100.0	100.0	100.0	100.0	100.0	100.0	100.0	100.0	100.0	100.0	100
1/2" (12.5mm)	100.0	100.0	100.0	100.0	100.0	100.0	100.0	100.0	100.0	100.0	100.0	100.0	82-100
3/8" (9.5mm)	83.0	100.0	72.8	100.0	100.0	100.0	100.0	100.0	100.0	100.0	100.0	100.0	86
No. 4 (4.75mm)	25.0	100.0	29.2	100.0	100.0	100.0	100.0	100.0	100.0	100.0	100.0	100.0	66 max
No. 8 (2.36mm)	3.0	100.0	1.8	100.0	100.0	100.0	100.0	100.0	100.0	100.0	100.0	100.0	20-30
No. 16 (1.18mm)	2.0	100.0	1.5	100.0	100.0	100.0	100.0	100.0	100.0	100.0	100.0	100.0	16-24
No. 30 (600um)	2.0	100.0	1.4	100.0	100.0	100.0	100.0	100.0	100.0	100.0	100.0	100.0	17
No. 60 (300um)	2.0	100.0	1.4	100.0	100.0	100.0	100.0	100.0	100.0	100.0	100.0	100.0	14
No. 100 (150um)	2.0	100.0	1.4	100.0	100.0	100.0	100.0	100.0	100.0	100.0	100.0	100.0	11
No. 200 (75um)	1.5	100.0	1.1	100.0	100.0	100.0	100.0	95.0	12.0	37.0	100.0	100.0	9
								90.0	17.0	28.6	100.0	100.0	7.5
Bulk Sp Gr	3.975	1.900	2.682	1.900	1.900	1.900	1.900	2.800	2.800	2.402	1.900	1.900	2.758
Absorption, %	1.70	1.90	6.46	1.90	1.90	1.90	1.90	1.90	1.90	1.90	1.90	1.90	0.65
													1.045
													1.24

SUMMARY OF SUPERPAVE GYRATORY DESIGN DATA

DATA for M-JRHL	AB, %MIX	Gmb	Gmm	Voids (Pa)	VMA	VFA	Vbe	Pbe	Fbe
MIX. 1	6.6	2.187	2.691	16.2	24.7	38.6	9.53	4.52	1.04
MIX. 2	8.0	2.208	2.688	14.0	24.8	48.2	10.71	5.09	1.00
MIX. 3	8.6	2.218	2.683	13.1	24.8	47.1	11.99	6.49	1.08
MIX. 4	7.0	2.229	2.634	12.0	24.8	51.5	12.81	6.99	1.08

DATA for M-des.	Gmb	Gmm	Voids (Pa)	VMA	VFA	Vbe	Pbe	Gas	Fba
MIX. 1	6.6	2.458	2.691	6.1	16.7	87.7	10.87	4.52	2.538
MIX. 2	8.0	2.478	2.688	3.5	16.6	77.6	12.03	5.09	2.533
MIX. 3	8.6	2.488	2.683	2.8	16.7	83.3	13.10	5.49	2.538
MIX. 4	7.0	2.488	2.634	1.4	16.8	91.0	14.39	5.99	2.540

OPTIMUM DESIGN DATA @ N=85	ABR	Gmb	Gmm	%VOIDS (Pa)	VMA	VFA	Gsb	TSR	RCY AB	Virgin AB	ABR
60	6.0	2.478	2.688	Target: 3.6	16.6	77.6	2.758	0.88	2.82	5.18	47.0

REMARKS LINE 1	REMARKS LINE 2
Hamburg & TSR Made With Warm Mix	BITUMINOUS MIXTURE ABE@ 2
Target: 3.6	HOURS @ 305

Hamburg Wheel Information
Sample No. Pases: 20000
Sample Wheel Depth: 1.87

TSR Information
Conditioned: 114.1
Unconditioned: 129.6
TSR: 0.88
CA Strip Rating: 2
FA Strip Rating: 2
Additive Prod #: 1
Additive Product Name: 1
Additive %: 1

90WMA1639

Lab Preparing Design: \_\_\_\_\_  
 Designing Lab Misc: CURCE1603  
 Designing Lab Name: STATE

Tested by: \_\_\_\_\_  
 Verified by: \_\_\_\_\_  
 Reviewed by: \_\_\_\_\_  
 Final Approval: \_\_\_\_\_